

Laboratory Data on Coarse-Sediment Transport for Bedload-Sampler Calibrations

United States
Geological
Survey
Water-Supply
Paper 2299



Laboratory Data on Coarse-Sediment Transport for Bedload-Sampler Calibrations

By D.W. HUBBELL, H.H. STEVENS, Jr.,
J.V. SKINNER, and J.P. BEVERAGE

U.S. GEOLOGICAL SURVEY WATER-SUPPLY PAPER 2299

DEPARTMENT OF THE INTERIOR
DONALD PAUL HODEL, Secretary

U.S. GEOLOGICAL SURVEY
Dallas L. Peck, Director



UNITED STATES GOVERNMENT PRINTING OFFICE: 1987

For sale by the Books and Open-File Reports Section, U.S. Geological Survey,
Federal Center, Box 25425, Denver, CO 80225

Library of Congress Cataloging-in-Publication Data

Laboratory data on coarse-sediment transport for bedload-sampler calibrations.

(U.S. Geological Survey water-supply paper ; 2299)

Bibliography: p. 30

Supt. of Docs. no.: I 19.13:2299

1. Sediment transport—Measurement. 2. Hydrological instruments—Calibration. I. Hubbell, David Wellington, 1925— II. Series.

TC175.2.L33 1986 627'.122 86-600009

CONTENTS

Abstract	1
Introduction	1
Acknowledgments	2
Bedload-sampler calibration facility	2
Bedload trap and recirculation system	2
Control and data-acquisition systems	3
Tested bedload samplers	3
Experimental procedure	5
Hydraulic and sedimentologic data	7
Sampled bedload-transport rates	8
Measured bedload-transport rates	9
Particle-size distributions	9
Measured bedload transport	12
Sampled bedload transport	14
Water discharge	20
Water-surface slope	20
Longitudinal streambed-surface elevation	22
Streambed slope	24
Energy slope	26
Depth	26
Fixed-location streambed-surface elevations	27
Summary	27
References cited	30
Metric conversion factors	31
Availability of data	Inside back cover

FIGURES

1. Schematic diagram of bedload-sampler calibration facility 3
2. Schematic views of *A*, Sediment-recirculating system and *B*, Automated weigh-pan system 4
- 3–10. Photographs showing:
 3. End view of weigh pans withdrawn from the trap 5
 4. Downstream view of sediment trap, weigh-pan support structure, and load cells 5
 5. Enclosed instrument console with weigh-pan-control, data-acquisition, and master-time systems 5
 6. Helley-Smith bedload samplers having standard nozzles 6
 7. Helley-Smith bedload samplers having modified nozzles 6
 8. *A*, Arnhem bedload sampler and *B*, Full-scale VUV bedload sampler 7
 9. Mobile sampling platform 7
 10. *A*, Sample-weighing apparatus and *B*, Measurement cart 9
- 11–18. Graphs showing cumulative relative-frequency distribution of bedload-transport rates from samples collected with:
 11. Helley-Smith sampler no. 1 11
 12. Helley-Smith sampler no. 2 11
 13. Helley-Smith sampler no. 3 11
 14. Helley-Smith sampler no. 4 11

15. Helley-Smith sampler no. 5	12
16. Helley-Smith sampler no. 6	12
17. The Arnhem sampler	12
18. The full-scale VUV sampler	12
19. Temporal records of bedload-transport rates, q_p , measured at weigh pan 4 during A, run 1 and B, run 3, with the 6.5-mm bed material	14
20. Cumulative relative-frequency distributions of bedload-transport rates measured at weigh pan 4	14
21. Variation of discharge coefficient with ratio of the head on the weir to the height of the weir crest above the flume floor	21
22. Variation of intercept values of C_d-h/W relations with height of the bed surface above the flume floor	22
23–26. Longitudinal profile of streambed-surface elevation during:	
23. Run 3 with the 6.5-mm bed material	24
24. Run 3 with the 2.1-mm bed material	25
25. Run 1 with the 23.5-mm bed material	25
26. Run 1 with the bed-material mixture	26
27–30. Temporal variation in streambed-surface elevation at the sampling location during:	
27. Run 5 with the 6.5-mm bed material	28
28. Run 3 with the 2.1-mm bed material	28
29. Run 1 with the 23.5-mm bed material	29
30. Run 1 with the bed-material mixture	29

TABLES

1. Information on tested bedload samplers	8
2. General operational schedule by day number	8
3. General information on samples collected with test samplers	10
4. Summary of data on measured bedload-transport rates	13
5. Summary of hydraulic variables and bedload-transport rates	15
6. Particle-size distribution of sediment samples from the streambed, weigh pans, and Y diffusor	16
7. Water- and streambed-surface elevations for slope determinations	23
8. Streambed-surface elevations at fixed locations	30

The use of trade names is for identification only and does not constitute endorsement by the U.S. Geological Survey.

Laboratory Data on Coarse-Sediment Transport for Bedload-Sampler Calibrations

By D.W. Hubbell, H.H. Stevens, Jr., J.V. Skinner, and J.P. Beverage

Abstract

A unique facility capable of recirculating and continuously measuring the transport rates of sediment particles ranging in size from about 1 to 75 millimeters in diameter was designed and used in an extensive program involving the calibration of bedload samplers. The facility consisted of a 9-foot-wide by 6-foot-deep by 272-foot-long rectangular channel that incorporated seven automated collection pans and a sediment-return system. The collection pans accumulated, weighed, and periodically dumped bedload falling through a slot in the channel floor. Variations of the Helley-Smith bedload sampler, an Arnhem sampler, and two VUV-type samplers were used to obtain transport rates for comparison with rates measured at the bedload slot (trap). Tests were conducted under 20 different hydraulic and sedimentologic conditions (runs) with 3 uniform-size bed materials and a bed-material mixture. Hydraulic and sedimentologic data collected concurrently with the calibration measurements are described and, in part, summarized in tabular and graphic form. Tables indicate the extent of the data, which are available on magnetic media. The information includes sediment-transport rates; particle-size distributions; water discharges, depths, and slopes; longitudinal profiles of streambed-surface elevations; and temporal records of streambed-surface elevations at fixed locations.

INTRODUCTION

In 1979, the U.S. Geological Survey began the data-collection phase of a comprehensive laboratory investigation to evaluate and calibrate several different types of bedload samplers. The study was conducted at the St. Anthony Falls Hydraulic Laboratory (SAFHL), University of Minnesota, in a large flume that had been modified to house a unique system for circulating bedload and continuously measuring the rate of bedload transport. In addition, other equipment systems were installed to facilitate the continuous monitoring and the rapid and accurate periodic measuring of various hydraulic and sedimentologic variables pertinent to the study.

Because of current interest in the Helley-Smith bedload sampler (Helley and Smith, 1971; Druffel and others, 1976; Emmett, 1980), the principal effort of the investigation was directed toward testing and evaluating full-scale variations of this type of sampler; six variations were exam-

ined to evaluate the effect of different nozzle expansions and entrance widths. Additionally, an Arnhem sampler (Waterloopkundig Laboratorium, 1949) was tested under several different conditions, and two versions of the VUV sampler (Novak, 1957) were tested to a limited extent.

During the investigation, 4 different bed materials were placed in the flume, and runs were made under 20 separate stationary hydraulic and sedimentologic conditions. Three of the bed materials were composed of particles that had been sieved to yield nearly uniform materials having median particle diameters of 2.1 mm (5 runs), 6.5 mm (6 runs), and 23.5 mm (5 runs). The fourth bed material was artificially created by combining prescribed proportions of the uniform materials to yield an approximately log-normal size distribution of particles from 1.4 to 32.0 mm (4 runs). Because of particle attrition due to fracturing within the system during the first three runs with the uniform 23.5-mm bed material, the size gradation of the bed material during the fourth run was analogous to that of a mixture; newly sieved 23.5-mm material was installed to replace the nonuniform material for the fifth run. The test runs were made in the following order: 6.5-mm bed material, 2.1-mm material, 23.5-mm bed material, and mixed bed material.

As many as six different samplers were used in each run to collect bedload samples for evaluating and calibrating the individual samplers. Except for several runs involving the Arnhem sampler, between 60 and 120 samples usually were collected by each sampler during each run to define sampled rates. Short-duration bedload-transport rates measured by the automated weigh pans were obtained during each run for comparison with the sampled rates.

In addition to measurements of bedload transport, data were collected continuously on water discharge and on streambed-surface elevations, near the centerline of the flume, at several longitudinal positions. Also, periodically, longitudinal profiles of streambed-surface elevation and water-surface elevation were defined concurrently throughout the experimental reach. Samples of material from the streambed and from the weigh pans were collected for particle-size analysis periodically during runs; additional samples were collected at the outlet of the sediment-return line during runs with the bed-material mixture.

These various data constitute a large body of hydraulic and sedimentologic information on the transport of bedload particles that range in size from about 1.0 mm to 32.0 mm. The data are unique, not only because of the wide range of particle sizes that were used in the investigation, but also because of the relatively large flow depths that were maintained in all runs and the extent to which spatial and temporal variations in many variables were measured. However, because suspended-sediment transport had to be inhibited, the experimental data characterize only hydraulic and sedimentologic conditions attendant with low to moderate bedload-transport rates. Also, because the experimental flume could not be tilted, a transition zone of nonuniform flow existed at the upper end of the channel. Statistical procedures had to be used to ascertain the reach of channel where the flow could be considered uniform.

This report explains in detail how the data were collected, synthesized, and organized as a data base. Because of the large number of individual values, measured transport rates and other kinds of data are stored on magnetic media. Complete replications of part or all of these data are available from the U.S. Geological Survey (see Availability of Data, inside back cover). Summaries that indicate the extent and character of the various data sets, as well as mean values of several common variables, are presented in tables in this report, and selected segments of the data are depicted in graphical form to illustrate the magnitude and variability of various quantities.

Acknowledgments

Funding for construction of the calibration facility and for the sampler calibration program was provided, in a large part, by the U.S. Environmental Protection Agency. In addition, the U.S. Army Corps of Engineers, St. Paul District, funded the initial designing of the facility and contributed a mobile conveyor belt, as well as space at the Twin Cities Army Ammunition Plant, New Brighton, Minn., for the preparation of bed material. Northern States Power Co. provided space in a spillway outside of the laboratory for storing used bed material. The Washington District office of the U.S. Geological Survey contributed some supplemental funds. The late Dr. A.G. Anderson, Director of SAFHL, guided the early design activity on the calibration facility. Dr. Anderson's enthusiasm for the facility and for the sampler calibration program provided important encouragement for the project. After Dr. Anderson's death, the facility was completed under the direction of Dr. R.E.A. Arndt, SAFHL Director, and Professor John Ripkin. Mr. Loren M. Bergstedt, SAFHL, designed the mechanical and hydraulic features of the facility and supervised construction. The success of the program attests to the quality of Mr. Bergstedt's effort. The authors sincerely appreciate the skill and dedication that the entire staff at SAFHL devoted to the project.

BEDLOAD-SAMPLER CALIBRATION FACILITY

Mechanical elements of the bedload-circulation system were designed and constructed by SAFHL personnel in accordance with project specifications. The system (figs. 1 and 2) was incorporated into the main laboratory flume, which is a rectangular concrete channel that has a fixed horizontal floor and which is 9 ft wide, 6 ft deep, and 272 ft long. Flows up to about 300 ft³/s can be diverted from the Mississippi River through a sluice gate, into a vertical entrance tunnel, and from there through a baffle section into the flume. Flow rate is controlled by the sluice gate, and an adjustable sharp-crested weir at the end of the flume is used to fix the depth of flow.

Bedload Trap and Recirculation System

The primary element of the system was an automated sediment trap situated beneath the floor of the channel. The entrance to the trap was an adjustable-width slot across the full width of the channel at a position, designated station 0, 213 ft downstream from the channel entrance and 59 ft upstream from the weir. The slot was divided laterally into seven 1.3-ft sections and was adjusted to an open width of 1.0 ft in the longitudinal direction. Seven box-shaped containers open at the top, called weigh pans, were located directly below the seven slot sections (fig. 3). The weigh pans were fitted with doors on the bottom that were opened and closed by hydraulically actuated cylinders. Each weigh pan operated independently and was suspended freely by rods that passed vertically upward through thin struts to triangular brackets above the channel. Each bracket, in turn, connected to a cylindrically shaped load cell (fig. 4) that continuously produced an output voltage proportional to the submerged weight of the weigh pan and its contents. Limit controls caused the pan doors to open, then close, whenever a preset voltage (weight) was reached. The weigh pans were suspended within a hopper section that was shaped at the bottom to form a tapered cylindrical channel that housed a hydraulically driven sediment-return feeder screw (auger). The auger discharged sediment into a sump on the outside of the hopper (fig. 2B). The sump was connected by a short length of 8-in. pipe to the suction side of a recessed-impeller, materials-handling pump. A vertical, rectangular, constant-level water tank extended directly upward from the sump. The discharge side of the pump connected to an 8-in. sediment-return pipe that terminated in an inverted Y-shaped diffusor at the upper end of the channel. The system was designed to continuously measure and recirculate bedload particles ranging in size from about 1 to 75 mm, at rates as high as about 4 lb/s/ft, and to discharge water diverted to the channel back into the river.

During operation of the flume, particles transported down the channel as bedload fell through the slot and accumulated in the weigh pans, while the water passed over the

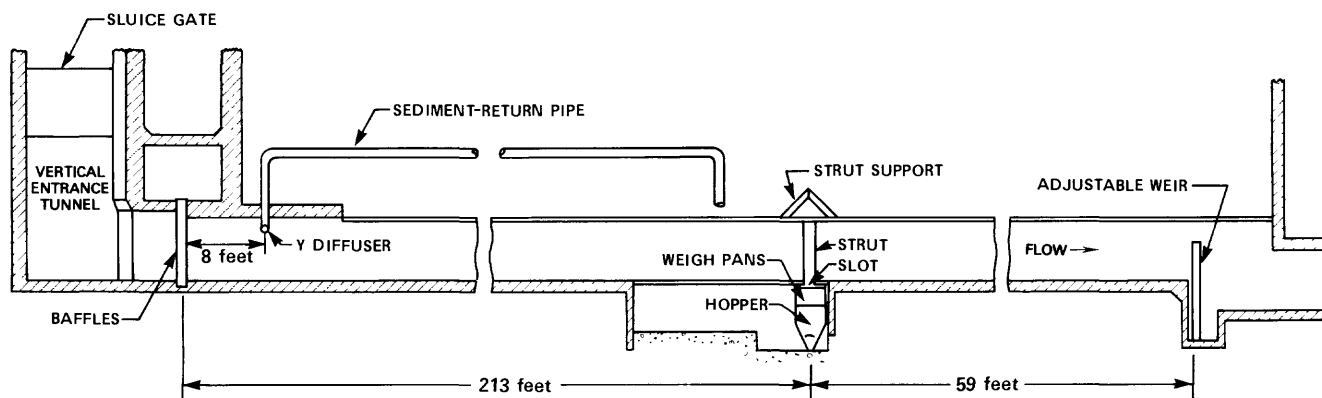


Figure 1. Schematic diagram of bedload-sampler calibration facility.

weir and out of the laboratory into large volumetric tanks that drain to the river. Whenever the weight of accumulated sediment in a weigh pan exceeded the preset level, the bottom doors opened and dumped the material onto the auger. The auger transported the material out of the hopper into the sediment-return sump. Clear water from the constant-level tank mixed with the sediment in the sump to produce a slurry that was pumped back to the upper end of the flume and discharged on either side of the centerline of the channel through the submerged Y diffuser. The water-surface elevation in the constant-level water tank was maintained equal to the water-surface elevation in the channel to minimize flow circulation vertically through the slot.

Control and Data-Acquisition Systems

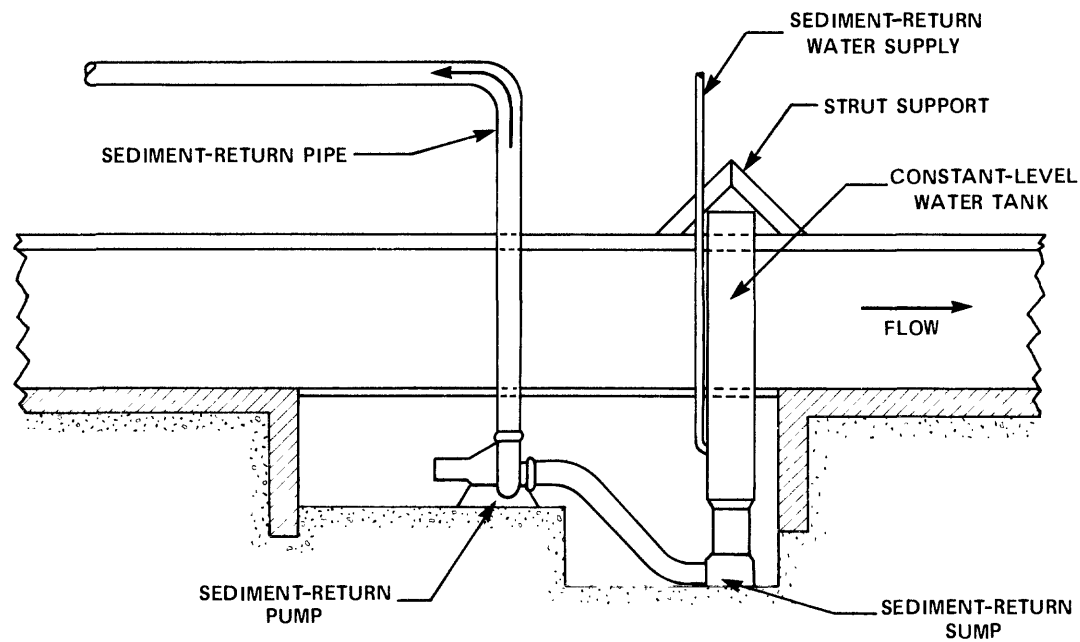
A system of relays actuated by the voltage output from the load cells controlled automatic dumping of the weigh pans. The electrical apparatus and override switches for this function, as well as an electronic time base for continuously documenting time to the nearest second and graphic and electronic data-acquisition instruments for recording the voltage outputs from the weigh-pan load cells, time, and several other variables, were housed in a movable, air-conditioned console (fig. 5). To facilitate determination of transport rates, output voltages from all load cells were graphed continuously on strip-chart recorders and were recorded digitally every 6 seconds on magnetic tape. The strip-chart records allowed the continual filling and dumping of the weigh pans to be monitored, whereas the digital data served as the primary record for transport-rate determinations.

TESTED BEDLOAD SAMPLERS

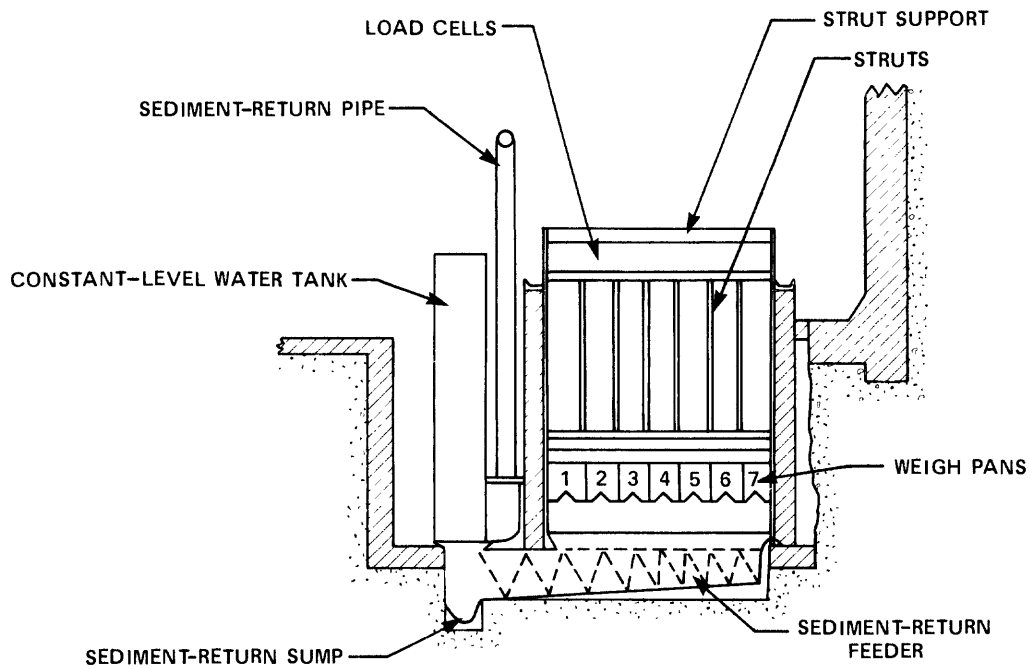
The Helley-Smith bedload sampler consists of an intake nozzle constructed of 1/4-in. steel or brass plate, a mesh sample bag that is attached at the rear of the nozzle,

and a supporting tubular-frame and tail assembly. The standard (original) nozzle consists of a straight, square entrance section, several inches long, welded to a tapered expansion section. The standard sample bag is 0.25-mm mesh constructed in the general shape of an elongated pyramid or cone. One standard nozzle has a 3- by 3-in. entrance (fig. 6A), and another has a 6- by 6-in. entrance (fig. 6B). Both standard nozzles have an area ratio, which is the ratio of the exit area to the entrance area, of 3.22. This degree of expansion gives the nozzles a hydraulic efficiency of about 1.54 (Druffel and others, 1976). Four modified nozzles, in addition to the standard nozzles, were fitted with standard sample bags and mounted into standard frames for testing. Two of the modified nozzles had 3- by 3-in. entrances, and two had 12- by 6-in. entrances (fig. 7). The expansion sections of all four modified nozzles flared very little compared to the standard nozzles; one nozzle of each size had an area ratio of 1.10, and the others had an area ratio of 1.40. In addition, a sampler having a standard 3- by 3-in. nozzle and frame, but a 0.5-mm mesh sample bag, was tested in one run; during the same run, a standard 3- by 3-in. sampler was used in an untethered condition.

A standard Arnhem sampler (fig. 8A) and a half-size, modified VUV sampler were provided by The Department of Minerals and Water Resources, Commonwealth of Canada, for testing. Both of these samplers were supported within a standard Arnhem frame. The unique feature of the frame (fig. 8A), which is used routinely with these samplers in the field, is a laterally mounted leaf spring that is intended to press the entrance nozzle of the sampler firmly onto the bed. Although the frame worked marginally satisfactorily with the Arnhem sampler, it apparently did not press the entrance of the VUV sampler against the bed. As a result, a disproportionate number of samples contained no material whatever. Because of the questionable validity of many samples collected with the half-size VUV, all samples were rejected and deemed unrepresentative. The other tested VUV sampler (fig. 8B) was a full-scale replica of Novak's (1957) original sampler, except that the tail section was not attached.



A



B

Figure 2. Schematic views of A, Sediment-recirculating system (side view) and B, Automated weigh-pan system (upstream view).



Figure 3. End view of weigh pans withdrawn from the trap; bottom doors are completely or partially open.

The numerical designation assigned to each sampler and special sampling arrangement are given in table 1. In addition, the table lists pertinent characteristics of the samplers and indicates the runs in which each sampler was tested.

EXPERIMENTAL PROCEDURE

The different bed materials used during the study were placed in the flume hydraulically by continuously feeding material into the sump, at the intake side of the pump, while the flume was in operation. The sediment was pumped to the upper end of the flume. There, it initially deposited, built up the bed, and then moved downstream as



Figure 4. Downstream view of sediment trap, weigh-pan support structure, and load cells.

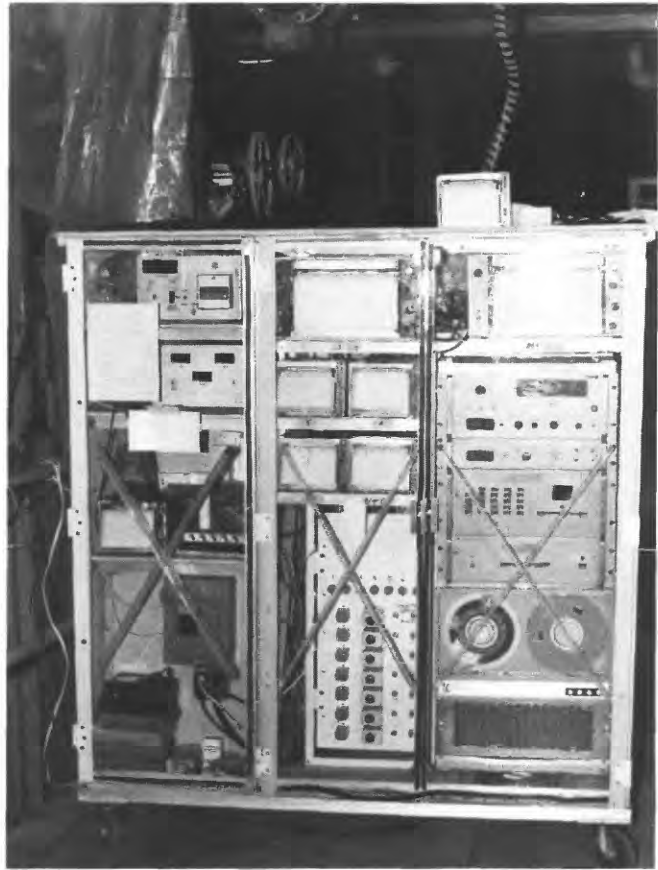


Figure 5. Enclosed instrument console with weigh-pan-control, data-acquisition, and master-time systems. Load-cell relays (lower center) and demodulators (hidden) controlled opening and closing of weigh-pan doors. Dual- and single-channel strip-chart recorders (upper center and upper right) monitored weigh-pan operation. Magnetic-tape, data-acquisition system (lower right) recorded cumulative time, sampling time, and voltage output from load cells that supported the weigh pans. Master-time system (upper left) generated cumulative and interval times.

the flow velocity and bed slope accommodated transport. Material was added until the depth of sediment at the lower end of the study reach was about 1.5 ft thick. The emplacement process ordinarily took about 12 hours.

For the first run, and each subsequent run thereafter, water discharge and height of the sharp-crested weir were adjusted to achieve and maintain, in a quasi-equilibrium state, the desired bedload-transport rate and flow depth. The period of adjustment required to reach stationarity varied from run to run. The duration of the flow-adjustment period (including emplacement of bed material) for all runs and all bed materials is given in table 2. In addition, table 2 lists the duration of the quasi-equilibrium period when the various data included in this report were collected. The periods are expressed in day numbers, which are a count of the number

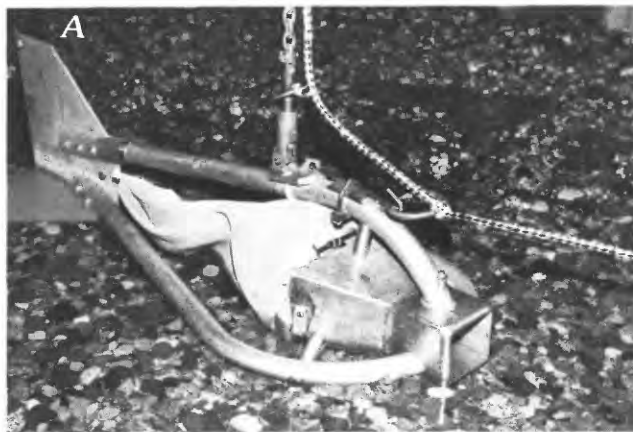


Figure 6. Helley-Smith bedload samplers having standard nozzles. A, 3- by 3-in. entrance; B, 6- by 6-in. entrance. Both nozzles have an area ratio of 3.22.

of full (8 to 9 hours) and partial (less than 8 hours) days when the flume was actually operating; consecutive day numbers do not necessarily represent consecutive calendar days.

Samplers being calibrated were stored on overhead tracks on a mobile sampling platform (fig. 9). The platform supported a high-speed chain hoist that could be moved to pick up and return samplers from storage and to raise and lower them at the downstream edge of the platform. A quick-release connector allowed samplers to be attached and detached rapidly from the hoist, and a quick-release tether (fig. 6A) prevented downstream drift during sampler placement and "scooping" during sampler retrieval. This arrangement facilitated sampling sequentially with a group of samplers (usually six) during a run so that the same hydraulic conditions and true bedload transport rates applied to all samplers in the group. That is, the samplers were used, one after the other, to obtain one or more samples from the cross section; then, after all samplers had been used, the sequence was repeated. Repetitions continued until the desired number of samples had been collected with each sampler. In runs 1-4 with the 6.5-mm bed material, each sampler was used

to collect three individual samples at lateral stations coincident with the centerlines of pans 2, 4, and 6; in all other runs with all bed materials, a single sample was collected with each sampler at center-channel, in line with the center of pan 4.

Individual samples and wet-sieved portions of samples were weighed in tared buckets under water to eliminate the necessity of drying samples. The submerged net weights of both samples and weigh-pan accumulations were corrected later to dry weights by multiplying by the ratio 2.65/1.65. The weighing apparatus, which consisted of a bottom-loading balance, a weighted table with a load-dampening release mechanism, and an immersion tank, is shown in figure 10A.

To calibrate the tested bedload samplers, transport rates, determined from the dry weight of individual samples collected in a known time and adjusted to a unit-width basis, were compared with true transport rates (dry-weight basis) determined from the calibration facility. Details of the calibration procedures are given by Hubbell and others (1985); the procedure involves comparison of rate distributions,



Figure 7. Helley-Smith bedload samplers having modified nozzles. A, 3- by 3-in. entrance; B, 12- by 6-in. entrance. Both nozzles have an area ratio of 1.1.

HYDRAULIC AND SEDIMENTOLOGIC DATA

Due to deposition of natural river sand in the vicinity of the sluice gate (fig. 1) outside of the laboratory, small concentrations of sand were continuously brought into the flume together with the water. All of this sand was finer than 1.414 mm, and 80 percent was finer than 1.0 mm. As a result, in all runs, natural river sand accumulated in the bed material and was transported as part of the bedload discharge. In addition, in runs in which the bed material contained gravel, some of the coarser particles were physically fractured by the auger and the recirculation system. This fracturing caused the quantity of coarse particles to decrease slightly and the quantity of particle fragments to increase slightly with the passage of time.

To eliminate the river sand and small fractured particles from the transport-rate determinations, all samples collected with the test samplers, except those obtained during runs with the bed-material mixture and during run 4 with the 23.5-mm material, were wet sieved to exclude particles finer than the lower limit of the size range of interest. Similarly, samples from the weigh pans were sized, and, in turn, weight accumulations in the weigh pans were reduced by the percentage of material finer than the designated separation size. All rates presented in this report, including the mean rate for each run, pertain only to the transport of particles coarser than the separation size used in the wet sieving. For reference, all tables that present or pertain to rate data specify the size range(s) to which the rates apply, and the section Particle-Size Distributions provides information on the percentages of excluded materials. Measured values of hydraulic variables that may be affected by the presence of sediment, of course, could not be adjusted to account for the effect of material excluded from the transport-rate data. Therefore, when considering these variables, the reader

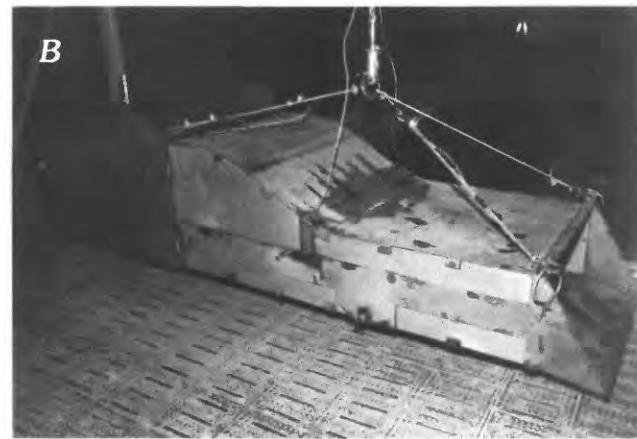
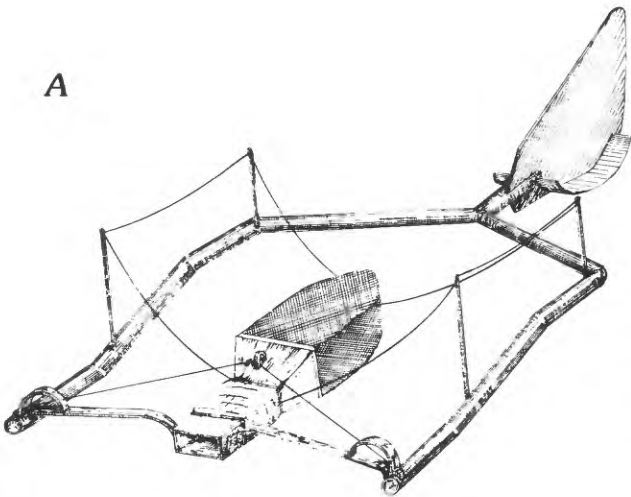


Figure 8. A, Arnhem bedload sampler and B, Full-scale VUV bedload sampler. The frame used in the tests to support the Arnhem sampler was similar to the one in the sketch. The full-scale VUV sampler was suspended by cables and was stabilized by dual tailfins, rather than by the normal tailpiece, and by tether lines fastened to rings at the top front of the sampler.

rather than comparison of individual rates or mean sample-set rates. Although continuous rates were determined every 6 seconds at all seven weigh pans, comparisons were made by using rates only from the pan or pans longitudinally inline with the sampling locations. Also, individual true rates (pan rates) were the mean rate during a composite period; composite periods usually corresponded to the sampling time used in each run (see p. 9).

Data for defining water discharge; water depth; water-surface, streambed, and energy slopes; bed configuration; and bed-surface elevation at fixed locations, including the sampling point, were measured concurrently with the sampling operation. Depths and bed-surface-elevation profiles were obtained with instrumentation (see p. 22) that was supported on a measurement cart (fig. 10B) situated upstream from the sampling platform.



Figure 9. Mobile sampling platform. Chain hoist mounted on superstructure of platform was maneuvered to retrieve, store, and raise and lower samplers; transducer probe with swivel head viewed the bed at sampler entrance.

Table 1. Information on tested bedload samplers

Identification number	Type	Intake nozzle entrance size ¹	Area ratio ²	Hydraulic efficiency	Runs in which sampler was tested with indicated type of bed material			
					6.5 mm	2.1 mm	23.5 mm	Mixture
1 ³ -----	HS ⁴	3 × 3	3.22	1.54	1-6	1-5	1-5	1-4
2-----	HS	3 × 3	1.10	⁵ 1.15	1-4	1-5	1-5	1-3
3-----	HS	3 × 3	1.40	⁵ 1.35	1-4	1-5	1-5	1-3
4-----	HS	12 × 6	1.10	⁵ 1.15	1-4	1-3	1-5	1-3
5-----	HS	12 × 6	1.40	⁵ 1.40	1-4	1-3	1-5	1-3
6 ³ -----	HS	6 × 6	3.22	1.54	1-6	1-5	1-5	1-3
7 ⁶ -----	VUV	19.9 × 7.9	—	1.00	—	—	—	4
8-----	Arnhem	3.4 × 2.0	3.07	1.00	5,6	4,5	3,5	—
11 ⁷ -----	HS	3 × 3	3.22	1.54	—	—	—	4
12 ⁸ -----	HS	3 × 3	3.22	1.54	—	—	—	4

¹Width × height, in inches.

²Ratio of nozzle exit area to entrance area.

³Standard design.

⁴HS, Helley-Smith.

⁵Estimated.

⁶Full-scale version.

⁷Not tethered.

⁸0.5-mm mesh bag.

needs to keep in mind that varying quantities of river sand and fractured material were mixed in the bed material and were in transport even though the nominal bed-material-size designations and presented rates do not reflect that fact.

Sampled Bedload-Transport Rates

Sampling variables changed somewhat during the course of the experimental program. The data in table 3

indicate, for each run with each bed material, which samplers were used, the order in which they were used, the number of samples collected with each sampler, the sampling location, the sieve separation size(s), and the data-file name. Sampling locations are identified by distance upstream from the trap (station 0). Transport rates determined from the samples are characterized in figures 11–18, which show, for each of the tested samplers during one run with each of the uniform bed materials, the cumulative relative-

Table 2. General operational schedule by day number

[Day number specifies the number of complete or partial days of actual flume operation; day number 1 is the first day on which the flow and weir height were adjusted either to load bed material into the flume or to establish conditions for a new run]

Type of bed material	Run number	Inclusive day numbers for indicated activity	
		Flow adjustment	Data collection
6.5 mm-----	1	1-9	10-17
	2	1-6	7-12
	3	1-2	3-9
	4	1-7	8-13
	5	1-8	9-14
	6	1-2	3-9
2.1 mm-----	1	1-4	5-12
	2	1-7	8-15
	3	1-2	3-9
	4	1-3	4-8
	5	1-5	6-12
23.5 mm-----	1	1-4	5-13
	2	1-2	3-8
	3	1-4	5-12
	4	1-2	3-7
	5	1-5	6-11
Mixture-----	1	1-5	6-12
	2	1-3	4-8
	3	1-2	3-8
	4	1	2-5

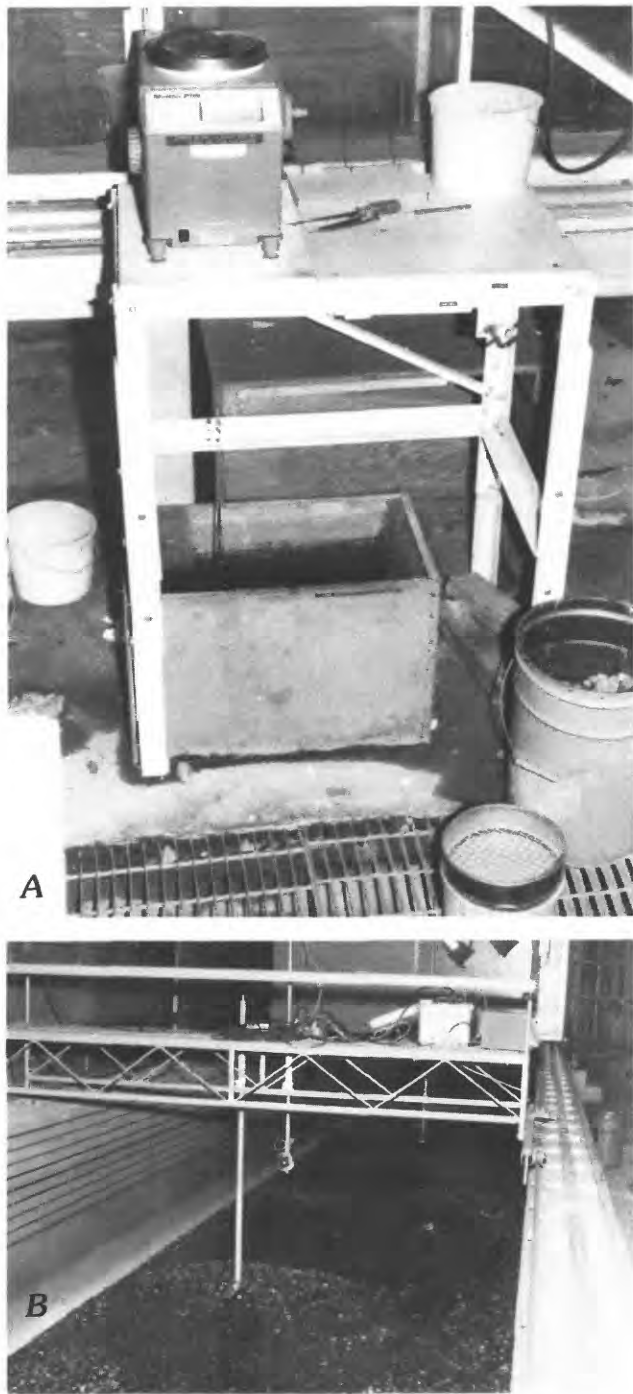


Figure 10. A, Sample-weighing apparatus. Tared buckets containing samples were suspended for weighing beneath the balance in the immersion tank. Handle of the load-dampening mechanism (right side of table) rotates to support or release positions. B, Measurement cart. Cart supported equipment for profiling bed-surface elevation longitudinally and for measuring velocity gradients vertically.

frequency distribution of sampled transport rates. The distributions demonstrate the typical extreme variations in sampled rates observed in all runs. Sampled rates, sampling

times, and other information for all samples collected in all runs are available on magnetic media (see Availability of Data, inside back cover) in data files named in the far right column of table 3.

Measured Bedload-Transport Rates

The true bedload-transport rate (bedload discharge) was determined directly as the time rate of change of weight in a weigh pan. Ordinarily, even though cumulative weights were recorded every 6 seconds, rates were averaged over periods, called composite periods, that were long enough to minimize the effects of force fluctuations on the weigh pans caused by turbulence in the flow above the slot and by pressure waves created by periodic dumping of the pans. The duration of the composite (averaging) period for a run was selected to correspond closely to the sampling time (time to collect an individual sample) used during the run. For each run with each bed material, the number of composite periods for which rates are available, the duration of the composite period, the mean transport rate measured at each weigh pan for the specified size range, and the data-file name are listed in table 4. Individual composite-period rates for all weigh pans, runs, and bed materials are available on magnetic media (see Availability of Data, inside back cover) in data files named in the far right column of table 4.

The most striking feature of the measured transport rates, as well as of the sampled rates, is their extreme and generally cyclic variation throughout time. Typical temporal records of measured transport rates during two different runs with the 6.5-mm bed material (fig. 19) exemplify these characteristics; similar variations were observed in all runs with all bed materials. The characteristics also are demonstrated indirectly in figure 20, which shows rates measured at weigh pan 4 in the same format and for the same runs as were used to present sampled rates in figures 11–18.

Mean bedload-transport rates measured in the cross section and measured at weigh pan 4 alone during the runs with each different bed material are presented in table 5, together with average values of pertinent hydraulic variables.

Particle-Size Distributions

Each of the uniform bed materials used in the experiments was prepared by sieving about 400 tons of commercial-grade sediments obtained from natural fluvial deposits. The sieving technique consisted of continually depositing unsieved material at the upper end of a 3- by 6-ft sieve screen that was mounted in a sloping position and vibrated at 60 Hertz. Particles retained on the screen were directed into one pile, and particles passing through the screen were directed to another pile. When two separations were required, the process had to be repeated.

Table 3. General information on samples collected with test samplers

[Run numbers appended with a or b designate continuation of the numbered run with a new complement of samplers. Particle-size analysis separation points: WS, wet sieve; DS, dry sieve]

Type of bed material	Run number	Longitudinal sampling station ¹ (feet)	Lateral sampling location by pan number	Sampling order by sampler number	Number of samples collected with each sampler	Particle-size analysis separation points (millimeters)	Data-file name
6.5 mm	1	28	2, 4, 6	6, 1, 2, 3, 4, 5	123	1.4 WS	SAMPDATA065R1
	2	28	2, 4, 6	6, 1, 2, 3, 4, 5	126	1.4 WS	SAMPDATA065R2
	2a	28, 68	4	1	236	1.4 WS	SAMPDATA065R2
	3	28	2, 4, 6	6, 1, 2, 3, 4, 5	120	1.4 WS	SAMPDATA065R3
	4	28	2, 4, 6	6, 1, 2, 3, 4, 5	120	1.4 WS	SAMPDATA065R4
	5	14, 28	4	1, 6	120	1.4 WS	SAMPDATA065R5
2.1 mm	5a	28	4	8	145	1.4 WS	SAMPDATA065R5
	6	28	4	1, 6	121	1.4 WS	SAMPDATA065R6
	6a	28	4	8	40	1.4 WS	SAMPDATA065R6
	1	28	4	6, 1, 2, 3, 4, 5	60	1.0 WS	SAMPDATA021R1
	2	28	4	6, 1, 2, 3, 4, 5	53	1.0 WS	SAMPDATA021R2
	3	10	4	6, 1, 2, 3, 4, 5	64	1.0 WS	SAMPDATA021R3
23.5 mm	4	10	4	1, 2, 3, 6	60	1.0 WS	SAMPDATA021R4
	4a	50	4	8, 3	40	1.0 WS	SAMPDATA021R4
	5	10	4	1, 2, 3, 6	69	1.0 WS	SAMPDATA021R5
	5a	27	4	8	40	1.0 WS	SAMPDATA021R5
	1	20	4	6, 1, 2, 3, 4, 5	81	11.3 WS	SAMPDATA235R1
	2	20	4	6, 1, 2, 3, 4, 5	80	11.3 WS	SAMPDATA235R2
Mixture	3	20	4	6, 1, 2, 3, 4, 5	60	11.3 WS	SAMPDATA235R3
	3a	20	4	8	40	11.3 WS	SAMPDATA235R3
	4	20	4	6, 1, 2, 3, 4, 5	74	16, 11.3, 8, 2 WS	SAMPDATA235R4
	5	20	4	6, 1, 2, 3, 4, 5	80	11.3 WS	SAMPDATA235R5
	1	20	4	6, 1, 2, 3, 4, 5	80	22.6, 16 WS; 11.3, 8, 5.6, 4, 2, 1 DS	SAMPDATA999R1
2.1 mm	2	20	4	6, 1, 2, 3, 4, 5	79	22.6, 16 WS; 11.3, 8, 5.6, 4, 2, 1 DS	SAMPDATA999R2
	3	20	4	6, 1, 2, 3, 4, 5	80	22.6, 16 WS; 11.3, 8, 5.6, 4, 2, 1 DS	SAMPDATA999R3
	4	28	4	7	80	22.6, 16 WS; 11.3, 8, 5.6, 4, 2, 1 DS	SAMPDATA999R4
2.1 mm	4a	28	4	11	61	22.6, 16 WS; 11.3, 8, 5.6, 4, 2, 1 DS	SAMPDATA999R4
	4b	28	4	12	80	22.6, 16 WS; 11.3, 8, 5.6, 4, 2, 1 DS	SAMPDATA999R4

¹Distance upstream from trap.²Collected alternatively at each station by moving back and forth.

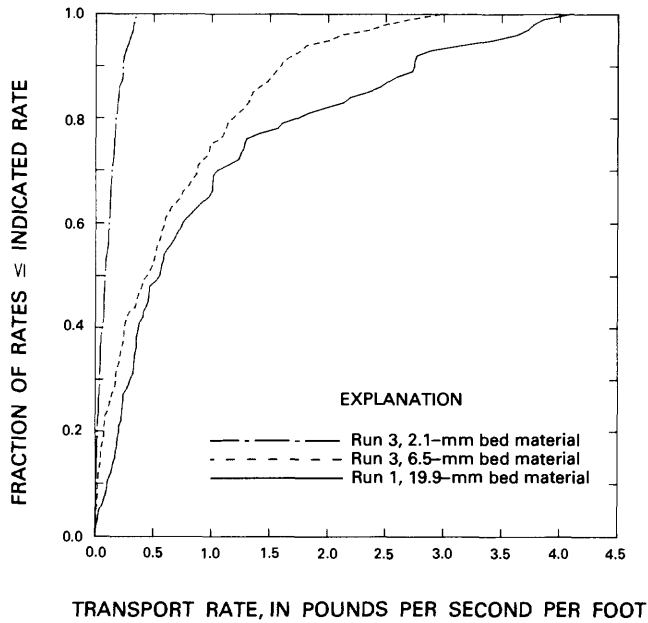


Figure 11. Cumulative relative-frequency distribution of bedload-transport rates from samples collected with Helley-Smith sampler no. 1.

The 6.5-mm material consisted of particles from a roofing-gravel mixture that had passed through an 8.0-mm, square-mesh screen. The 2.1-mm material was derived from No. 10 washed filter rock and was composed of particles that were retained by a 1.5-mm, square-mesh screen but which passed through a 2.5- by 6.4-mm, rectangular-mesh screen. Particles from a coarse gravel mixture that were retained by a 12.7-mm, square-mesh screen, but which

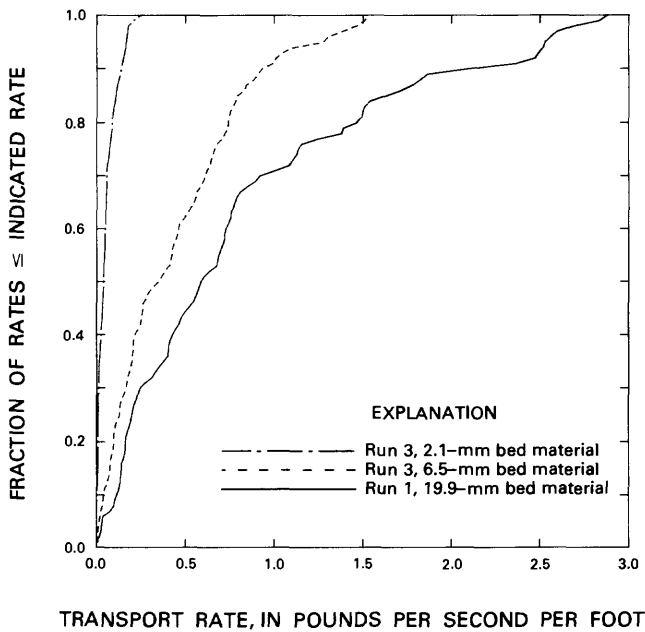


Figure 12. Cumulative relative-frequency distribution of bedload-transport rates from samples collected with Helley-Smith sampler no. 2.

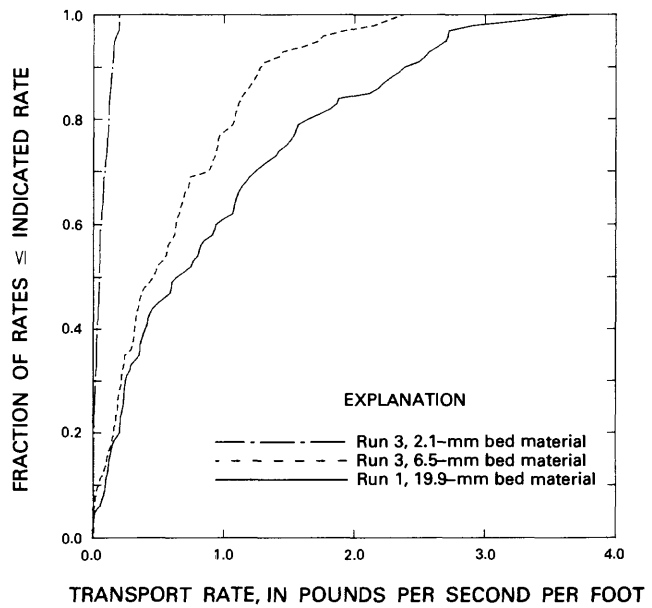


Figure 13. Cumulative relative-frequency distribution of bedload-transport rates from samples collected with Helley-Smith sampler no. 3.

passed through a 32.0-mm, square-mesh screen, composed the 23.5-mm bed material. The bed-material mixture was produced by combining particles removed from the flume after the sixth run with 6.5-mm material and after the fifth run with 23.5-mm material, together with 2.1-mm material that had been prepared but never used; the proportions of the mix, by volume, were 11, 3, and 4, respectively.

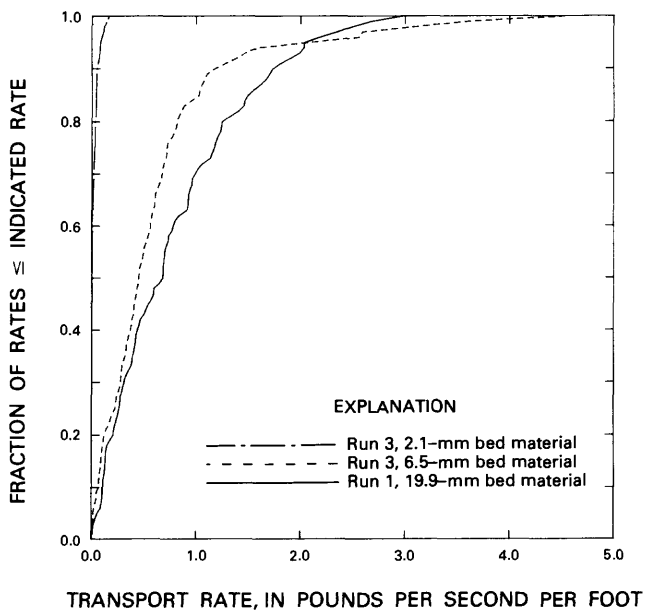


Figure 14. Cumulative relative-frequency distribution of bedload-transport rates from samples collected with Helley-Smith sampler no. 4.

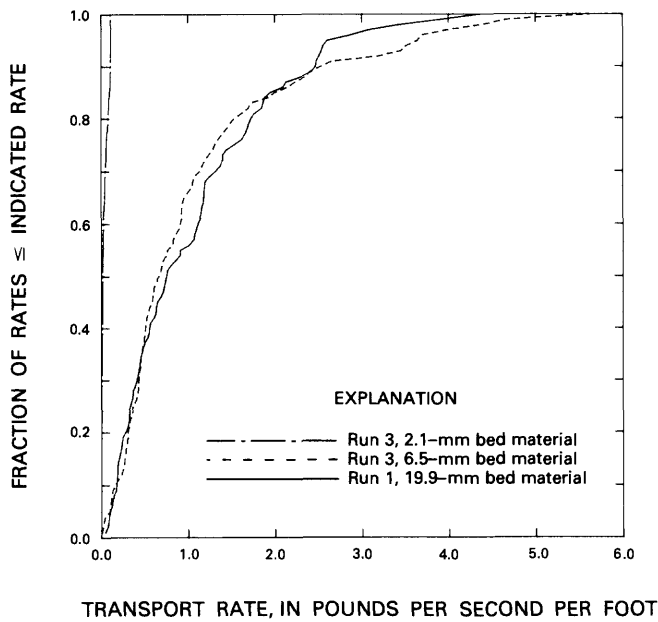


Figure 15. Cumulative relative-frequency distribution of bedload-transport rates from samples collected with Helley-Smith sampler no. 5.

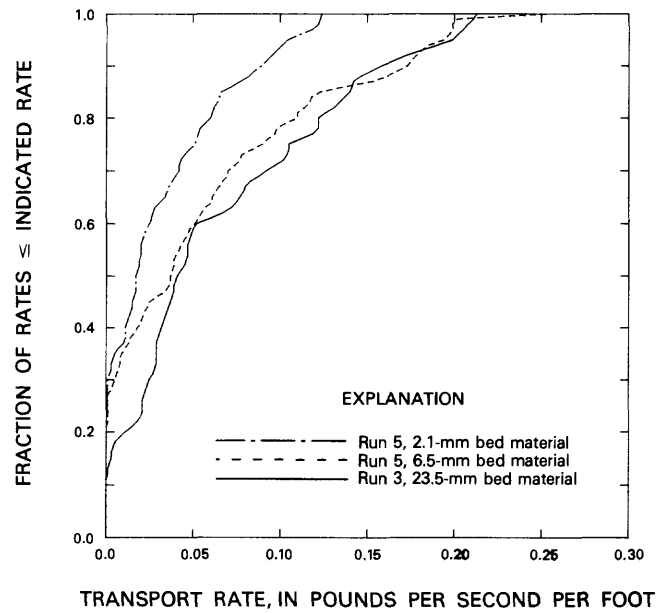


Figure 17. Cumulative relative-frequency distribution of bedload-transport rates from samples collected with the Arnhem sampler.

Measured Bedload Transport

The particle-size distribution of material in transport was determined by analyzing samples that were collected from the weigh pans and from the streambed surface after the water had been drained from the flume. During runs with the 6.5- and 23.5-mm materials, the entire size distribution of each sample was defined. However, with the 2.1-mm

material, in addition to defining the entire size distribution of regularly collected samples, the percentage of river sand finer than 1.0 mm in a number of extra samples also was determined. For the mixture runs, in addition to weigh-pan and streambed samples, material discharged back into the upper end of the channel through the Y diffuser was collected and analyzed frequently.

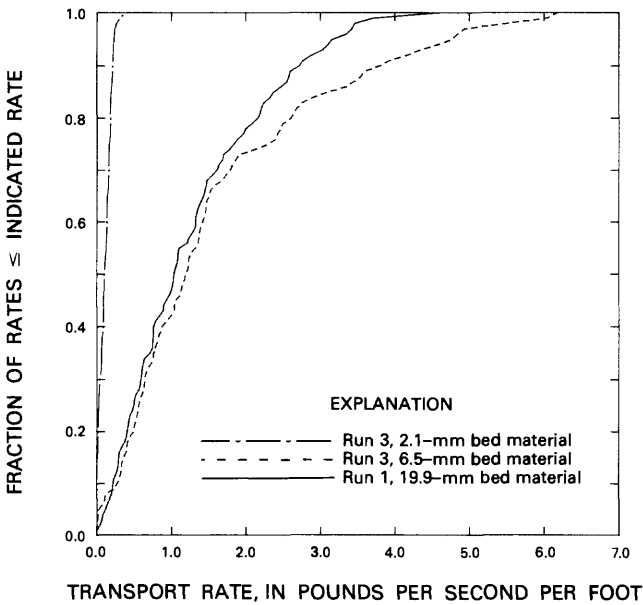


Figure 16. Cumulative relative-frequency distribution of bedload-transport rates from samples collected with Helley-Smith sampler no. 6.

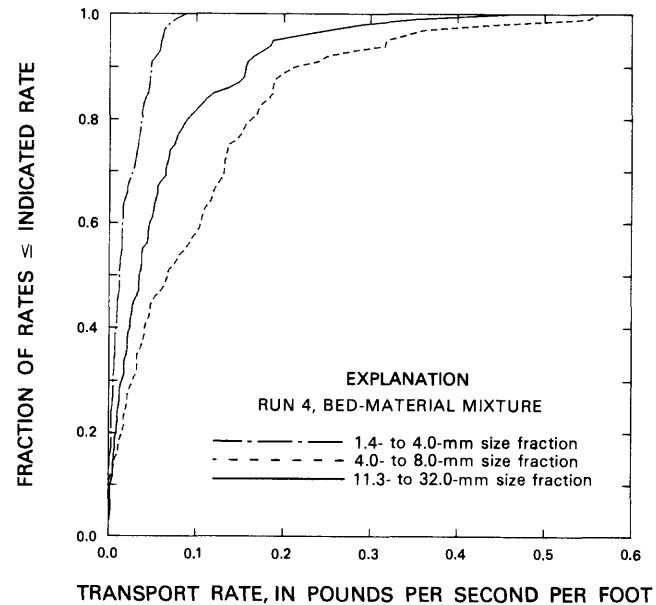


Figure 18. Cumulative relative-frequency distribution of bedload-transport rates from samples collected with the full-scale VUV sampler.

Table 4. Summary of data on measured bedload-transport rates
 [Listed number of composite periods is the maximum possible for each weigh pan during the indicated run]

Type of bed material	Run number	Number of composite periods	Duration of each composite period (seconds)	Particle-size range (millimeters)	Mean bedload-transport rate for indicated weigh pans (pounds per second per foot)							Data-file name
					1	2	3	4	5	6	7	
6.5 mm	1	1,354	120	>1.4	0.047	0.064	0.072	0.068	0.062	0.060	0.047	TRAPRATE065R1
	2	3,140	42	>1.4	.277	.335	.357	.360	.348	.365	.277	TRAPRATE065R2
	3	3,553	36	>1.4	.332	.435	.489	.496	.477	.471	.359	TRAPRATE065R3
	4	679	180	>1.4	.049	.060	.065	.070	.066	.067	.050	TRAPRATE065R4
	5	1,845	48	>1.4	.111	.129	.131	.107	.108	.099	.102	TRAPRATE065R5
	6	1,242	100	>1.4	.006	.018	.019	.014	.015	.015	.007	TRAPRATE065R6
2.1 mm	1	1,252	120	>1.0	.049	.056	.058	.053	.052	.040	.044	TRAPRATE021R1
	2	829	210	>1.0	.034	.037	.038	.034	.033	.032	.033	TRAPRATE021R2
	3	1,062	120	>1.0	.073	.084	.082	.071	.066	.096	.058	TRAPRATE021R3
	4	502	300	>1.0	.013	.014	.015	.012	.012	.012	.010	TRAPRATE021R4
	5	1,394	120	>1.0	.029	.033	.036	.033	.032	.033	.028	TRAPRATE021R5
23.5 mm	1	10,866	18	>11.3	.554	.730	.919	.928	.921	.889	.601	TRAPRATE235R1
	2	3,468	36	>11.3	.200	.254	.313	.266	.274	.281	.183	TRAPRATE235R2
	3	1,900	84	>11.3	.067	.110	.132	.108	.117	.093	.051	TRAPRATE235R3
	4	6,920	18	all sizes	.651	.744	.831	.798	.752	.761	.665	TRAPRATE235R4
	5	5,621	25	>11.3	.283	.346	.447	.507	.462	.332	.312	TRAPRATE235R5
Mixture	1	3,904	35	all sizes	.242	.240	.260	.251	.224	.259	.255	TRAPRATE999R1
	2	2,082	60	all sizes	.156	.156	.164	.154	.134	.160	.144	TRAPRATE999R2
	3	1,295	100	all sizes	.095	.101	.113	.088	.081	.104	.092	TRAPRATE999R3
	4	2,263	30	all sizes	.322	.340	.350	.328	.284	.355	.341	TRAPRATE999R4

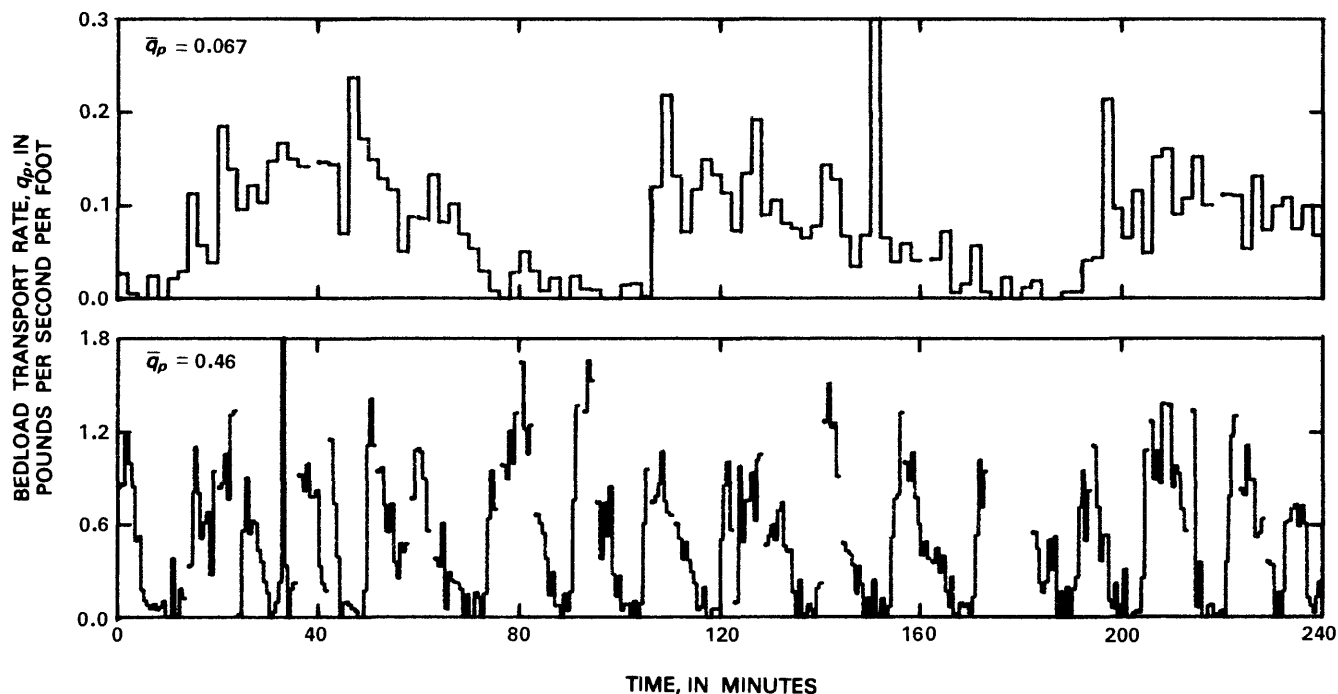


Figure 19. Temporal records of bedload-transport rates, q_p , measured at weigh pan 4 during A, run 1 and B, run 3, with the 6.5-mm bed material. The mean transport rate for the part of the record depicted in each graph is given in the upper left corner. Discontinuities in the record represent weigh-pan dumps.

Particle-size distributions of all samples collected during the uniform-bed-material runs, as well as size distributions of the raw unprocessed material, recombinations of samples from stock piles of the excluded (reject) material, and the retained material placed in the flume, are presented in table 6. The distributions are expressed both in terms of the whole sample (designated "all sizes" in table 6) and the part coarser than the finest separation size (the part to which sampled and measured rates pertain). Because many analyses were made during runs with the bed-material mixture, only size distributions defined near the first and last day of each run with the mixture are given in table 6. Change in size with time of operation can be assessed by referring to the day number of each distribution.

Particle-size data from runs with the uniform bed materials are compiled only in tabular form. However, the size distributions of all streambed, weigh-pan, and Y-diffusor samples from the mixture runs are available on magnetic media (see Availability of Data, inside back cover) in a data file named PARTSIZE999RA.

Sampled Bedload Transport

Except for run 4 with the 23.5-mm material, samples collected during runs with uniform bed materials ordinarily were not analyzed to define their size distribution. However, most unanalyzed samples were wet sieved to determine the percentage of material finer than the specified separation size. For unsieved samples, the percentage of material finer than the separation size for each sampler was

taken as the average from sieved samples collected during the run with that sampler. For run 4 with 23.5-mm material and for runs with the mixture, all samples were completely sized either by wet sieving or by a combination of wet and dry sieving (see table 3). Available size information was used, in turn, to determine, for each sample, the transport rate(s) of the size range(s) of interest.

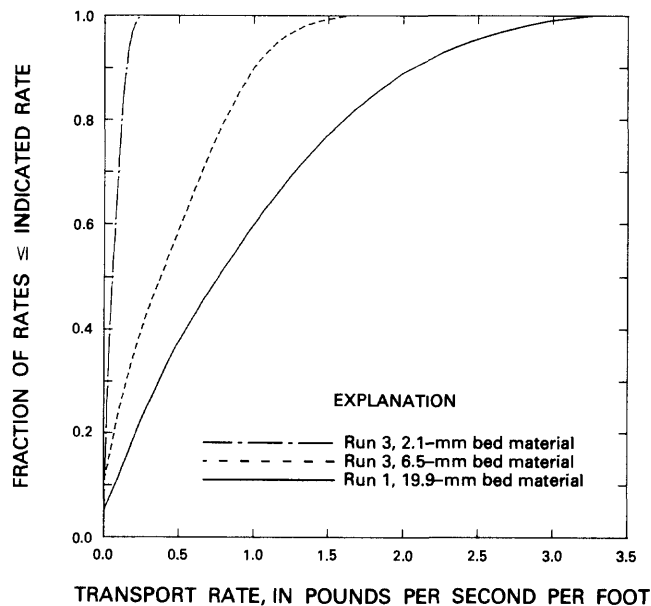


Figure 20. Cumulative relative-frequency distributions of bedload-transport rates measured at weigh pan 4.

Table 5. Summary of hydraulic variables and bedload-transport rates

Type of bed material	Run number	Mean water discharge (cubic feet per second)	Mean velocity (feet per second)	Mean depth (feet)	Mean slope (feet/foot)		Energy	Particle-size range (millimeters)	Mean bedload-transport rate (pounds per second per foot)	
					Streambed	Water surface			Flume cross section	Weight pan 4
6.5 mm	1	141.6	3.98	3.95	(1)	0.000914	(1)	>1.4	0.060	0.068
	2	133.0	4.68	3.16	0.00298	.00216	0.00206	>1.4	.331	.360
	3	182.5	5.13	3.95	.00332	.00220	.00238	>1.4	.437	.496
	4	154.6	4.29	4.00	.00140	.000854	.000788	>1.4	.061	.070
	5	89.2	4.05	2.45	.00209	.00166	.00170	>1.4	.112	.107
	6	114.1	3.19	3.97	.000313	.000455	.000410	>1.4	.013	.014
2.1 mm	1	110.0	3.47	3.52	.000935	.000970	.000956	>1.0	.050	.053
	2	90.4	2.88	3.49	.00144	.000827	.00106	>1.0	.035	.034
	3	108.7	3.53	3.42	.00285	.00107	.00121	>1.0	.076	.071
	4	86.7	2.84	3.39	.00485	.000907	.000754	>1.0	.012	.012
	5	106.8	3.43	3.46	.00328	.000928	.00107	>1.0	.032	.033
23.5 mm	1	213.3	7.43	3.19	.00249	.00320	.00280	>11.3	.792	.928
	2	194.0	6.04	3.57	.000416	.00132	.00113	>11.3	.253	.266
	3	172.6	5.31	3.61	.000600	.000610	.000782	>11.3	.097	.108
	4	207.5	6.55	3.52	.00229	.00151	.00146	all sizes	.743	.798
	5	203.8	7.14	3.17	.00228	.00207	.00230	>11.3	.384	.507
Mixture	1	140.6	4.69	3.33	.00167	.000706	.000727	all sizes	.247	.251
	2	129.6	4.24	3.40	.00148	.000524	.000435	all sizes	.153	.154
	3	113.3	3.77	3.34	.00141	.000430	.000348	all sizes	.096	.088
	4	141.8	4.82	3.27	.00322	.000835	.00114	all sizes	.331	.328

¹Not well defined.

Because of the numerous size analyses and wet-sieve separations that were made of samples collected with the test samplers, no size information is presented in this report in tabular form. However, defined analysis data and assigned percent-finer values for all samples are stored on magnetic media in the SAMPDATA file for each run (see table 3 for complete data-file names). These data are available on request (see Availability of Data, inside back cover).

Water Discharge

The constant water discharge established for each run was attained during an adjustment period at the beginning of each run by varying the height of the weir at the end of the flume and the opening of the sluice gate at the upper end of the flume to achieve the desired flow depth and bedload-transport rate. Sufficient time was allowed between significant adjustments for the bed slope to change and reach a quasi-equilibrium state. After desired transport and depth states were established and the data-collection period was in progress, the sluice gate and weir settings remained nominally fixed, except during startup at the beginning of each day and shutdown at the end of each day. However, during most runs, the sluice gate had to be adjusted slightly now and then to compensate for changes in river elevation at the intake structure, and during several runs, weir height had to be adjusted to maintain a reasonably constant flow depth and bedload-transport rate.

The water-surface elevation at a point about 25 ft upstream from the weir was continuously monitored by an electronic water-stage recorder mounted over a stilling well on the outside wall of the flume. The recorder's voltage output, which is proportional to water-surface elevation, was graphed continuously by a strip-chart recorder. Periodically during each run, output voltages were read directly from the recorder and noted on the strip-chart record to provide adjustment factors for correcting the pen trace.

The relation between stage (water-surface elevation) and discharge was established through calibrations based on measurements of the flow volume accumulated during periods of several minutes. Six sets of calibration data were collected during the course of run sequences with the four different bed materials. For each set, a series of discharges was established by sequentially adjusting the sluice-gate opening. For each discharge, voltages from the stage recorder were read and recorded both manually and via a strip-chart recorder while flow was accumulated to near the top of one of two 15,000-ft³ tanks outside of the laboratory. The mean flow rate for each gate setting was determined from the measured volume and time of accumulation.

Analysis of the sets of calibration data indicated that discharge varied with stage, weir height, and thickness of bed material in the flume. The dimensionless weir discharge coefficient, C_d , is plotted in figure 21 against the ratio of the

head on the weir, h , to height of the weir crest above the channel bottom, W , for each set of calibration data. The discharge coefficient was computed from:

$$Q = 2/3 C_d b h \sqrt{2gh} \quad (1)$$

where Q is discharge,

b is the channel width, and

g is the gravity constant.

Also shown in figure 21 are linear regression lines that represent each set of calibration data. Although the slopes of all lines are not precisely the same, they are sufficiently close that a single slope of 0.1534 can be used to characterize all data sets. By averaging the intercept values of lines having a slope of 0.1534 that pass through each point of a data set, an overall intercept was established for each data set. The average intercept values plotted against H_b , the height of the bed surface above the flume floor, are presented in figure 22. Values of H_b for both the calibrations and the individual runs were determined by deducting the mean depth of flow from the difference between the mean water-surface elevation at station 20 (upstream from the slot) and the elevation of the flume floor.

Differences between discharges measured during the calibrations and counterpart discharges computed using the relations depicted in figures 21 and 22 average 0.06 percent and have a standard deviation of 0.81 percent. Mean water discharges for each run listed in table 5 are believed to be within about 2 percent of the true mean discharge.

Water-Surface Slope

Water-surface elevations were measured by using manometers. A series of nine piezometer tubes that connected to a common manometer board extended upstream from the bedload trap (station 0) and terminated in screened outlets that were cemented along the centerline of the horizontal flume floor every 20 ft from station 20 to station 180. Bed material covered the outlets. All manometers were read simultaneously at intervals throughout each run. The number of sets of readings that were used to compute the average water-surface slope for each run is listed in column 3 of table 7. Many, but not all, of the sets of readings were obtained concurrently with longitudinal streambed-surface elevation profiles to facilitate computations of total depth.

Because of (1) the relatively deep depths and high flow velocities attendant in many of the runs, (2) the presence of vertical struts at the slot (station 0), and (3) flow expansion due to the absence of bed material downstream from the slot, water-surface slopes were not uniform throughout the length of the flume. To exclude data obtained from parts of the channel where slopes were not uniform, water-surface elevations were subjected to statistical analysis. For each run, every set of water-surface elevations was used to determine the water-surface slope for a base reach

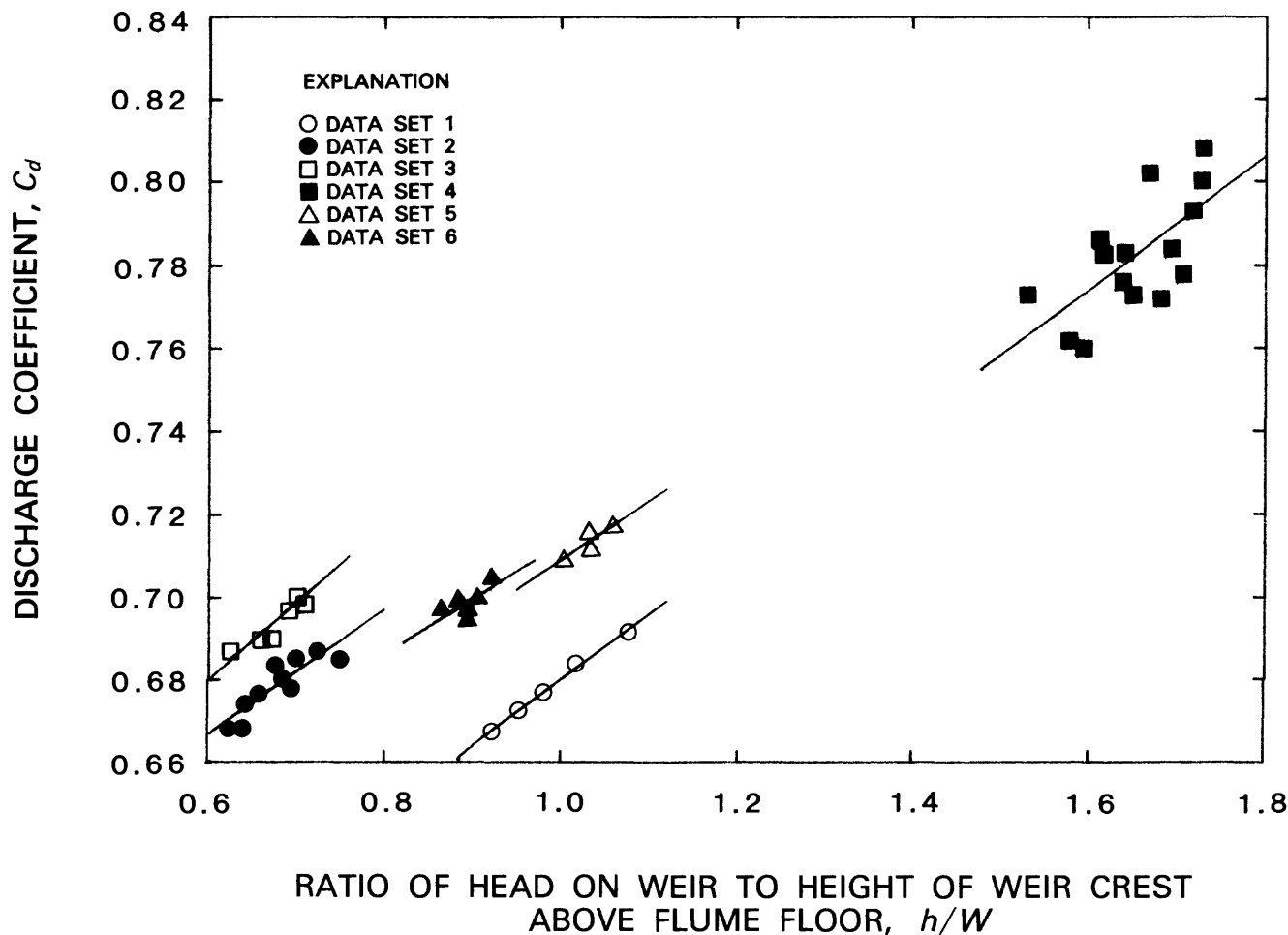


Figure 21. Variation of discharge coefficient with ratio of the head on the weir to the height of the weir crest above the flume floor. Each regression line represents a different set of calibration data.

between stations 20 and 40 (upstream from the slot). Slopes for the base reach then were compared statistically, at confidence coefficients of 90 and 95 percent, with counterpart slopes for reaches adjacent to the base reach to ascertain whether or not the slopes of the adjacent reach were likely to be from the same slope population as those for the base reach. If so, elevations from the adjacent reach were included with elevations from the base reach to form a new base reach, and slopes for the new, longer base reach were redetermined by linear regression. These slopes, in turn, were compared with slopes from the next adjacent reach to establish if all slopes were part of the same population. This process of extending the length of the base reach was continued until it was evident that the slopes for the adjacent and base reaches were different. The average slope for the run was then taken as the average of the least-squares slopes from all sets of elevations for the base reach.

The analysis procedure is based on the premise that changes in slope occur abruptly between the uniform and nonuniform reaches, rather than gradually throughout the entire reach. Although the premise cannot be verified be-

cause of the considerable variations in slopes, graphs of all computed average slopes, which also were used in making judgments about the commonality of slopes, indicate that slope changes in the water surface usually were reasonably abrupt.

The data in columns 4 and 5 of table 7 indicate, for each run, the stationing of the end points of the reach for which a uniform slope was presumed to exist; table 5 lists the mean slope values for all runs. For those few runs in which relatively long reaches of common slope were separated by a short reach of dissimilar slopes, the average slope was determined by using elevations from the entire reach.

The precise degree to which computed mean water-surface slopes represent uniform-flow conditions cannot be estimated reliably. However, on the basis of variances of the slope sets used to define the mean slope for each run, most mean slope values (see column 7 of table 5) can be expected (99-percent confidence coefficient) to be well within 25 percent of the true mean slope, except for slopes for the 23.5-mm runs, which may be somewhat less accurate.

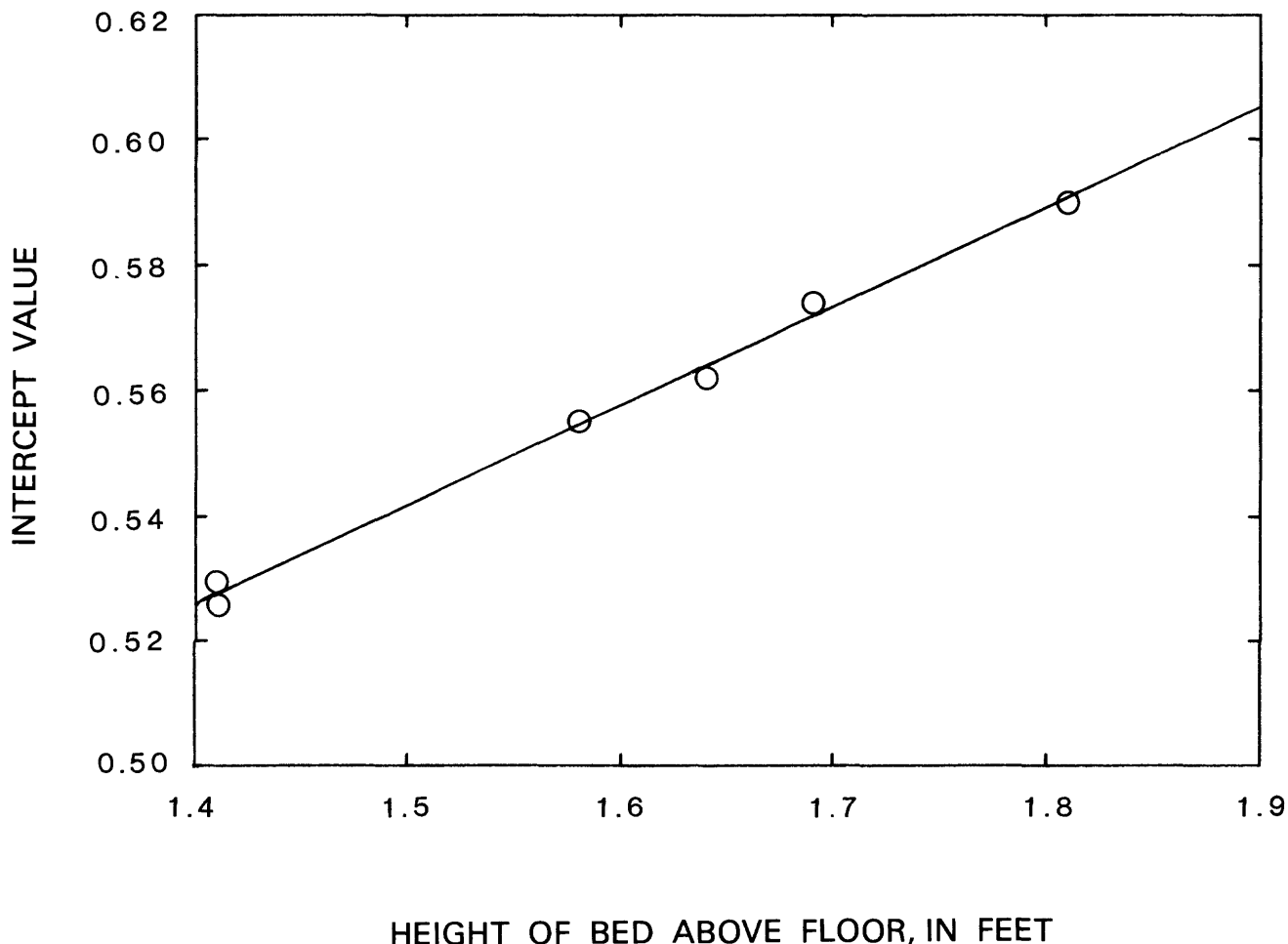


Figure 22. Variation of intercept values of C_d-h/W relations with height of the bed surface above the flume floor. C_d , dimensionless weir discharge coefficient; h , head on the weir; W , height of the weir crest above the channel bottom.

Water-surface elevations are available on magnetic media (see Availability of Data, inside back cover) in the files named in column 6 of table 7. The elevation datum is the horizontal flume floor.

Longitudinal Streambed-Surface Elevation

Streambed-surface elevations along the channel were measured periodically during each run by means of an ultrasonic sounder (fathometer) capable of measuring distance to the nearest 0.01 ft. The sounder's voltage output, which is proportional to the distance between the transducer face and the bed, was graphed on a strip-chart recorder. The transducer probe was mounted on the mobile measurement cart (fig. 10B) at a lateral position coincident with the centerline of the channel; the transducer was submerged about 15 in. The cart traversed the length of the channel along horizontal steel rails. One wheel of the cart was constructed with a milled recess at the outside. A microswitch contact mounted on the cart was actuated with every revolution of the wheel. Each switch closure produced a tick mark on the graphic

recorder indicative of 0.4713 ft of travel. Longitudinal profiles of the streambed-surface elevation were obtained by moving the measurement cart to the upstream end of the channel and then manually pushing the unit slowly downstream while the sounder produced a continuous graphic record of depth below the transducer face and the progression of tick marks delineated horizontal distance. The sounder was calibrated at the beginning and end of most days to define slight shifts in the parameters of the linear relation between voltage and distance.

The graphic records of all profiles were digitized and then converted by using calibration curves to provide values of actual distance between the transducer face and the streambed at intervals of about 0.15 ft along the measured reach. The exact lengths of the intervals varied, depending on the recorder chart speed and the rate of movement of the cart, because digitized values were automatically read every 0.03 in. along the graphic record. The variable-interval data, in turn, were converted by interpolation between the distance marks to transducer-to-streambed distances every 0.2 ft along the measurement reach. Because the transducer

Table 7. Water- and streambed-surface elevations for slope determinations

Type of bed material	Run number	Water-surface slope				Streambed slope				Energy slope			
		Number of water-surface elevation sets	Reach stationing ¹ (feet)		Data-file name	Number of bed-surface elevation profiles	Reach stationing ¹ (feet)		Data-file name	Number of pairs of water- and bed-surface elevations	Reach stationing ¹ (feet)		
			Start	End			Start	End			Start	End	
6.5 mm	-- 1	25	40	100	WATERELV06SR1	14	(2)	(2)	PROFBDEL06SR1	14	(2)	(2)	
	2	27	20	100	WATERELV06SR2	14	50	120	PROFBDEL06SR2	14	50	120	
	3	25	20	100	WATERELV06SR3	13	50	120	PROFBDEL06SR3	13	50	120	
	4	26	20	100	WATERELV06SR4	9	50	120	PROFBDEL06SR4	9	50	110	
	5	30	20	100	WATERELV06SR5	8	40	120	PROFBDEL06SR5	8	40	120	
	6	10	20	100	WATERELV06SR6	8	40	110	PROFBDEL06SR6	7	40	120	
2.1	----- 1	11	20	120	WATERELV02IR1	10	40	120	PROFBDEL02IR1	10	40	120	
	2	19	20	140	WATERELV02IR2	16	40	120	PROFBDEL02IR2	16	60	120	
	3	23	40	180	WATERELV02IR3	12	30	130	PROFBDEL02IR3	12	30	130	
	4	16	40	180	WATERELV02IR4	14	30	130	PROFBDEL02IR4	14	30	130	
	5	19	40	180	WATERELV02IR5	17	40	130	PROFBDEL02IR5	16	30	130	
23.5	----- 1	20	20	180	WATERELV23SR1	17	40	140	PROFBDEL23SR1	17	40	140	
	2	9	20	180	WATERELV23SR2	9	40	140	PROFBDEL23SR2	9	40	130	
	3	19	20	180	WATERELV23SR3	19	40	140	PROFBDEL23SR3	19	40	140	
	4	15	20	180	WATERELV23SR4	8	40	120	PROFBDEL23SR4	8	30	110	
	5	16	20	180	WATERELV23SR5	13	30	130	PROFBDEL23SR5	12	30	130	
Mixture	-- 1	19	20	180	WATERELV999R1	19	30	130	PROFBDEL999R1	19	30	130	
	2	23	20	180	WATERELV999R2	21	30	130	PROFBDEL999R2	21	30	130	
	3	18	20	180	WATERELV999R3	18	40	120	PROFBDEL999R3	18	30	120	
	4	10	20	180	WATERELV999R4	10	40	120	PROFBDEL999R4	10	40	130	

¹Distance upstream from trap.

²Not well defined.

face for each profile remained horizontal along the measurement reach, the transducer-to-streambed distances could be converted directly to streambed elevations. The elevation datum is the horizontal flume floor.

All converted streambed-elevation profiles, which define streambed configuration along the centerline of the measurement reach, are available on magnetic media (see Availability of Data, inside back cover) under the file names given in column 10 of table 7. The start and ending stations given in columns 8 and 9 of table 7 do not define the extent of the measurement reach for which the profile data are available. Rather, the stations pertain to the reach for which streambed slopes were defined. Most profiles extend for at least 100 ft. Typical profiles during high-rate runs with each of the different bed materials are illustrated in figures 23–26. Similar configurations were observed in all runs with all bed materials.

Streambed Slope

Because the streambed slope usually was not uniform along the entire length of the measurement reach, streambed slopes were determined in virtually the same manner as water-surface slopes. That is, for each run, a base reach near the downstream end of the measurement reach was selected, and bed slopes for the reach were determined by linear regression from the streambed-surface elevations defined every 0.2 ft. For most runs, the base reach had to be at least 30 ft long to average out the extreme variations created by

the bed forms. The slopes of the base reach were then compared statistically with similarly determined slopes for an adjacent reach to test whether or not the slopes of the adjacent reach were from the same slope population as those of the base reach. If they were, elevations from each profile for the base and adjacent reach were joined and used to define, by linear regression, a set of slopes for a new and longer base reach. These slopes, in turn, were compared with slopes from the next adjacent reach to extend the reach length until the slopes of the base and adjacent reaches were deemed to be from different slope populations. The average slope for the run was then taken as the average of the slopes for the final base reach.

In most runs, the heights of the bed forms exceeded the average elevation change throughout the slope reach. Consequently, computed streambed slopes for a given reach often differed substantially from one another, depending on the relative positions of the bed forms at the upstream and downstream ends of the reach. To reduce the differences, fairly long reaches were tested and later combined with the base reach. As a result of the relatively long reaches and the moderately large variances in slopes computed for base and adjacent reaches, real differences may be masked in the analysis to the degree that the slope computed for some final base reaches is not truly a uniform slope but is a composite of different slopes. This possibility can cause substantial errors in streambed slopes.

The number of profiles used to determine the mean streambed slope for each run and the beginning and ending

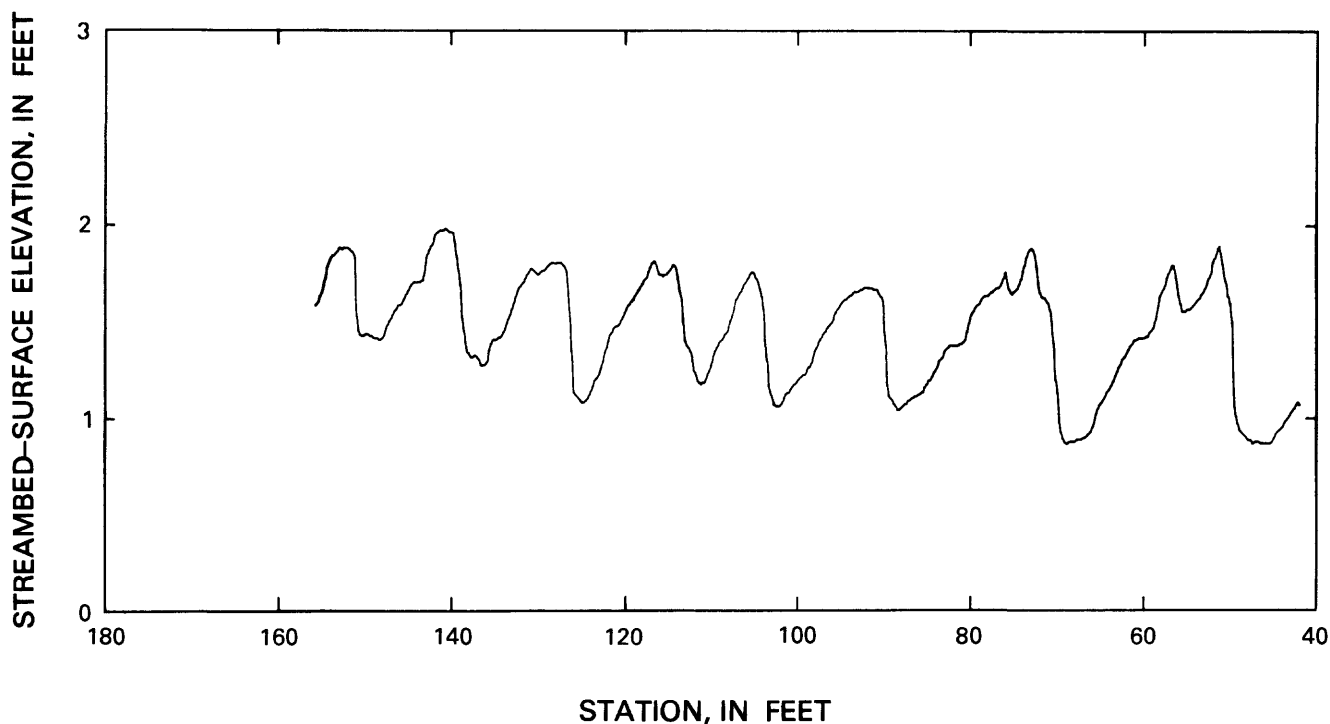


Figure 23. Longitudinal profile of streambed-surface elevation during run 3 with the 6.5-mm bed material.

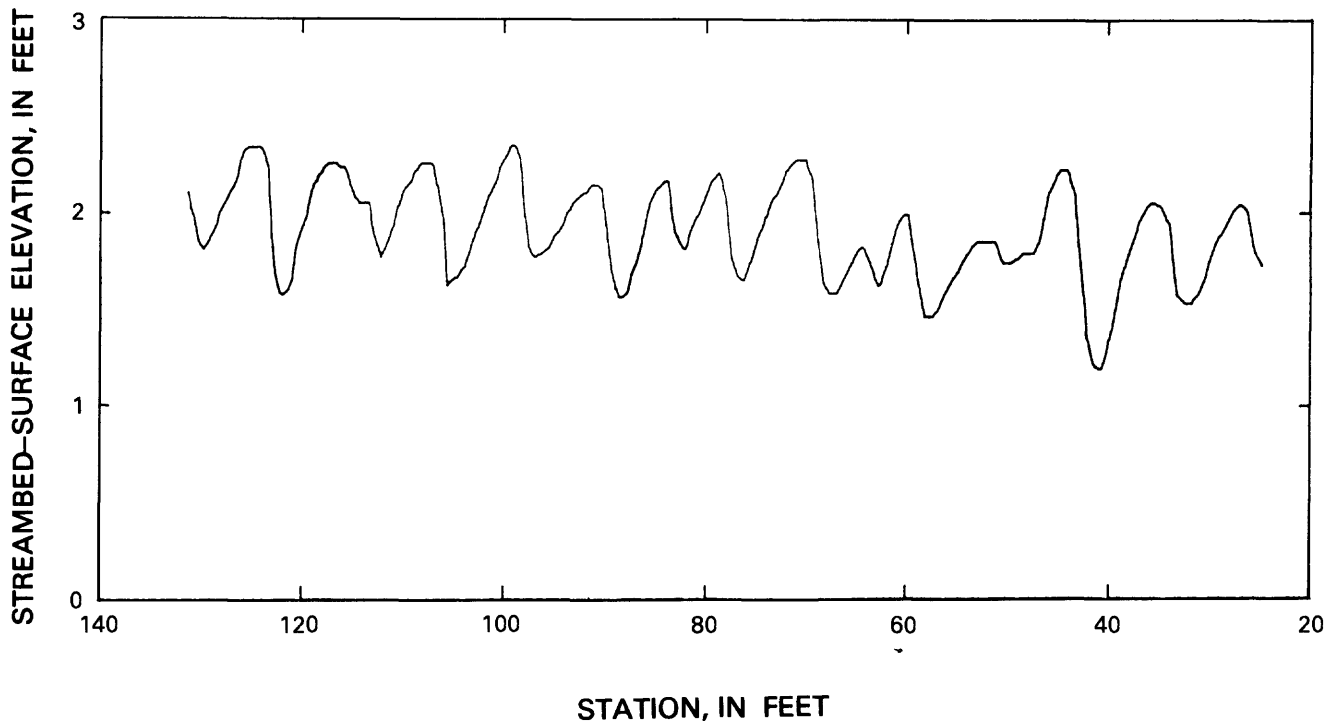


Figure 24. Longitudinal profile of streambed-surface elevation during run 3 with the 2.1-mm bed material.

stations of the final base reach are listed in columns 7-9 of table 7. The computed mean streambed slope for each run is given in table 5. A comparison of mean streambed and water-surface slopes for each run (see table 5) suggests that

in some runs the flow may have been nonuniform throughout the slope reach. For example, in run 4 with 2.1-mm material, the difference between mean depths at the downstream and upstream ends of the slope reach computed from

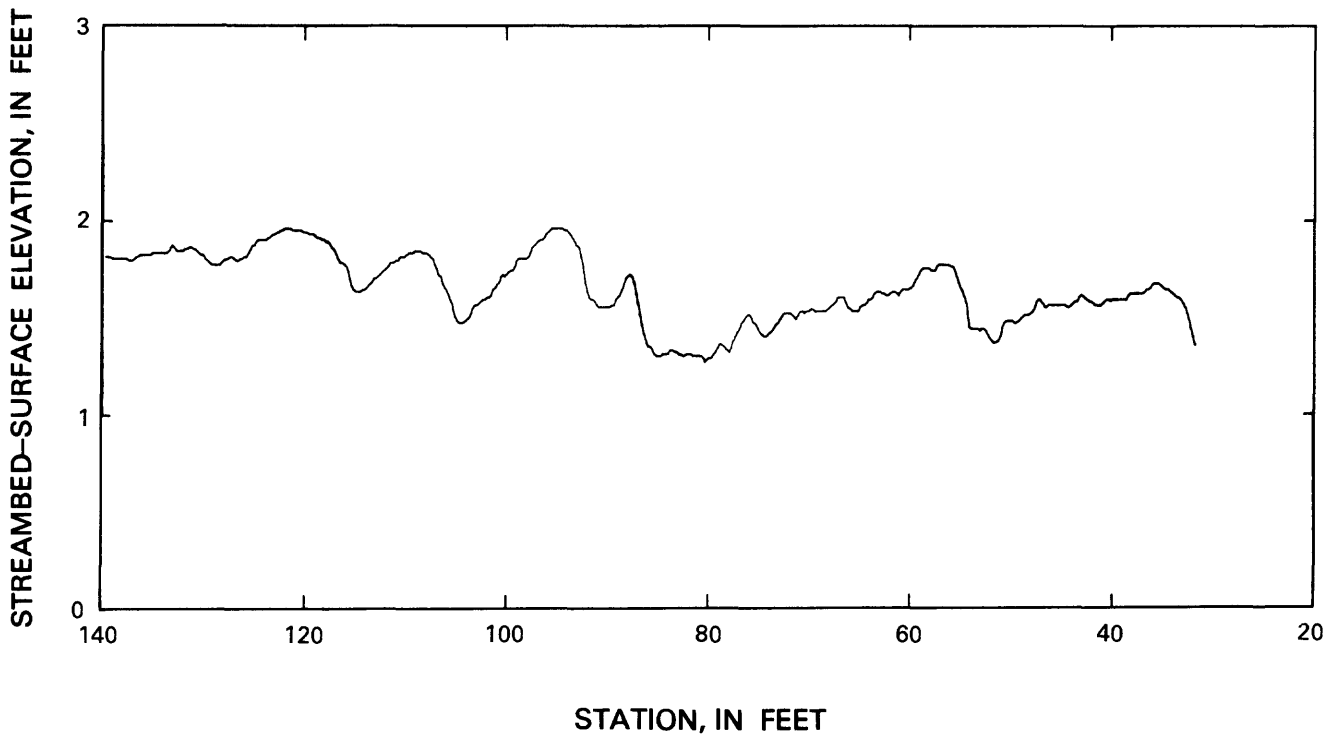


Figure 25. Longitudinal profile of streambed-surface elevation during run 1 with the 23.5-mm bed material.

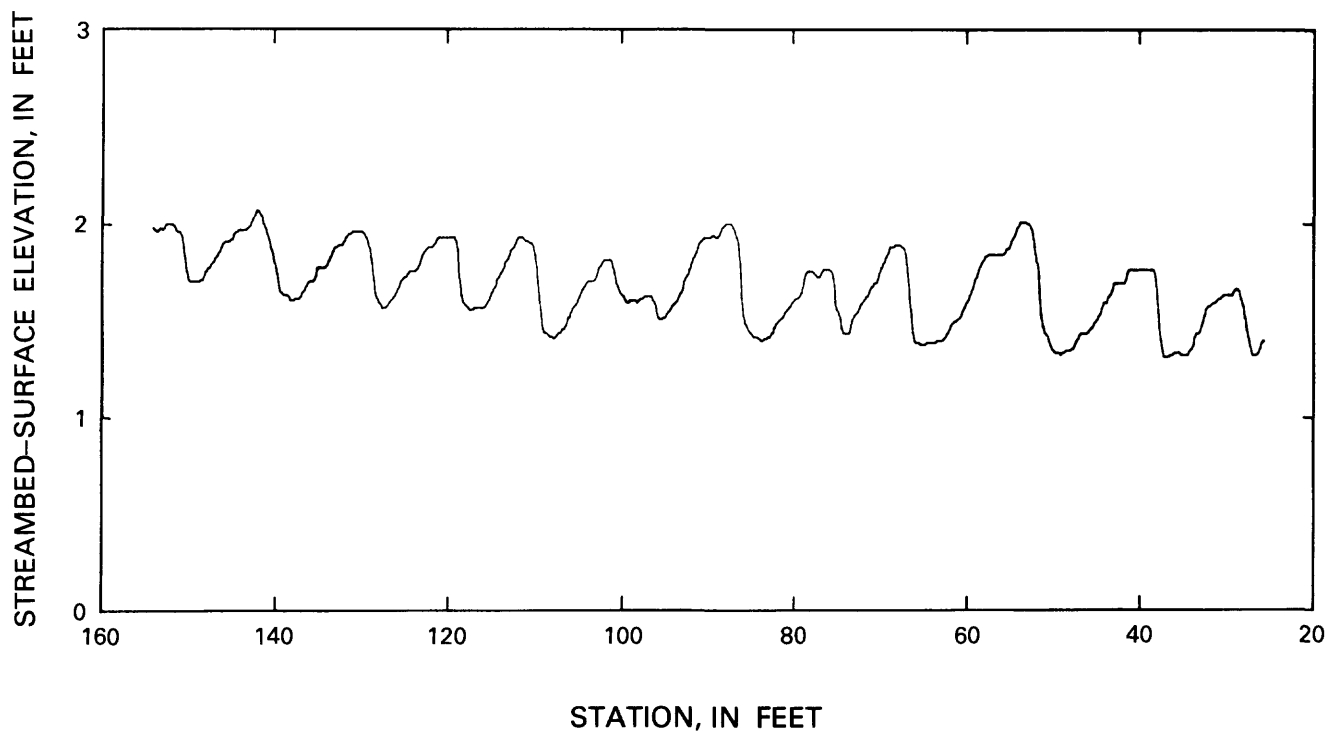


Figure 26. Longitudinal profile of streambed-surface elevation during run 1 with the bed-material mixture.

these slopes was 0.39 ft. This difference indicates decelerating flow. In contrast, a comparable depth difference computed by trial from mean water-surface and energy slopes (table 5) indicates slightly accelerating flow. For two other runs with 2.1-mm material and for one run with the bed-material mixture, depth differences computed from streambed and water-surface slopes were about 0.2 ft. Counterpart depth differences, however, from comparisons of water-surface and energy slopes were only several thousandths of a foot. Because of the potential for relatively large errors in streambed slopes, and the similarity between water-surface and energy slopes, it seems reasonable to assume that the flow was uniform throughout the slope reach during all runs.

Energy Slope

The energy slope for each run was computed by using water discharges and the pairs of water-surface and streambed-surface elevations that had been measured concurrently during the run. These data were combined by applying the continuity and Bernoulli equations to yield, for each elevation pair, the relative energy of the flow every 0.2 ft along the length of the reach for which both water-surface and streambed-surface elevations had been defined. The method was as follows: (1) Depths were determined at 0.2-ft intervals along the channel from the difference between corresponding water-surface and streambed-surface elevations; (2) velocity heads were computed at 0.2-ft inter-

vals from the depths and from the instantaneous discharge per unit width that existed when the pair of elevations were measured; and (3) depths, velocity heads, and corresponding potential heads (measured from the horizontal flume floor) were summed to yield relative total energy every 0.2 ft. The total energy values then were used to determine energy slopes by the same procedure as had been used to compute water-surface and streambed slopes. For most runs, the stationing of the final base reach was the same as or corresponded closely to that for the final streambed-slope reach. Because of the extreme variations in bed elevation and the necessity to determine water-surface elevations by interpolation between defined points located 20 ft apart, final energy slopes may be slightly less accurate than water-surface slopes. As a result, computed energy slopes probably do not reflect the true uniform energy gradient as precisely as does the water-surface slope.

The number of pairs of water-surface and streambed-surface elevations used to determine the energy slopes in each run and the stationing of the final slope reach are given in columns 11–13 of table 7. The computed mean energy slope for each run is listed in table 5.

Depth

Mean depth for each run was determined by averaging mean depths computed from the pairs of concurrent streambed- and water-surface profiles measured during the run. The mean depth from each pair of profiles was obtained

by averaging the 0.2-ft-interval depths that also were used for the energy-slope determinations. Rather than average all such depths available from each profile pair, or perform statistical tests to determine which depths should be averaged, only depths within the reach between stations 40 and 100 were included in the averaging process. Possibly the most reasonable procedure would have been to average depths for the same reach for which each energy slope was defined. However, the energy computations required water discharges that could be computed only with a knowledge of mean depth (see equation 1 and associated explanation); hence, mean depths had to be computed first for some arbitrary reach. The length of the reach between stations 40 and 100 is sufficiently long for the bed-form undulations to be adequately averaged out, and, with the exception of several profiles, the reach is included within the final reaches used for the energy-slope determinations. Computed mean depths for all runs are listed in table 5. These depths are estimated to be within 2 percent of the actual mean depth in the measurement reach.

Fixed-Location Streambed-Surface Elevations

Streambed-surface elevations at the sampling locations were monitored continuously during runs 5 and 6 with the 6.5-mm material and runs 1 and 2 with the 2.1-mm material. Soundings were made by using an ultrasonic sounder similar to the one used for longitudinal profiling; however, the transducer head was rotated from the vertical so that the distance to the bed was measured diagonally. The position of the head permitted the transducer probe to be mounted offcenter and out of the way of the sampling equipment, but to focus on the streambed directly in front of each sampler's nozzle (see fig. 9).

In all other subsequent runs, streambed-surface elevations were measured at the sampling points and in the center of the channel at station 5. Soundings at the sampling point also were obtained with the transducer head rotated and the probe mounted offcenter; soundings at station 5 were vertical. Because only two ultrasonic sounders were available, and at times, only one of the two channels in each sounder was operative, measurements had to be interrupted whenever longitudinal profiles were obtained. For purposes of analysis, an effort was made to continue measurements at the sampling point whenever possible. As a result, records at the sampling point usually are somewhat more extensive than those at station 5.

All graphic records were digitized and converted, by using appropriate voltage-distance calibration curves, to transducer-to-streambed distances. In the digitizing process, distances were determined at a fixed length interval along the graphic record. Then, by applying the exact chart speed, chart distances were converted to time, and transducer-to-streambed distances were determined, by interpolation,

every 18 seconds. The transducer-to-streambed distances measured at the sampling point subsequently were corrected to represent vertical distances by dividing by $\cos A$, where A is the angle between the transducer face and a horizontal plane. Finally, the vertical distances were adjusted to correspond to streambed-surface elevations relative to the horizontal flume floor.

Typical records collected at the sampling locations for the different bed materials are shown in figures 27–30. Each record was obtained during the run having the highest bedload-transport rate, except for the 6.5-mm bed material. For all runs, the magnitude, frequency, and character of changes in streambed elevation at station 5 virtually were the same as those at the sampling station, regardless of where the sampling station was located. Information, by bed material and run, on the duration of all streambed-surface elevation records from fixed locations is presented in table 8. The records are available on magnetic media (see Availability of Data, inside back cover) from the files named in table 8.

SUMMARY

A unique facility for measuring bedload transport in a large laboratory flume was used in an extensive program of calibrating bedload samplers. The facility, which was situated at St. Anthony Falls Hydraulic Laboratory, was designed to continuously measure the transport rate of bedload ranging in size from about 1 to 75 mm. The primary elements of the facility were automated weighing pans, located beneath the channel, which continuously weighed bedload falling through a slot (trap) in the floor, and an auger-pump assembly, which circulated sediment back to the upstream end of the channel. Six versions of the Helley-Smith bedload sampler, an Arnhem sampler, and two VUV-type samplers were used to sample transport rates for comparison with rates measured at the trap.

For the investigation, three uniform bed materials and a bed-material mixture were installed in the flume, and 20 different flow and transport conditions were established. Detailed hydraulic and sedimentologic data collected during the various runs with the several bed materials include sampled and measured bedload-transport rates; particle-size distributions of sediment in transport and in the streambed; water discharges; water depths; water-surface, streambed, and energy slopes; longitudinal profiles of streambed-surface elevations; and temporal records of streambed-surface elevations at the sampling point and at a fixed location close to the trap. These data are available, on magnetic media, for general distribution and use (see Availability of Data, inside back cover). Detailed descriptions explain how the data were collected and synthesized, and tables indicate the extent of the data and how the data are filed for access by computer. Summary tables provide mean values of im-

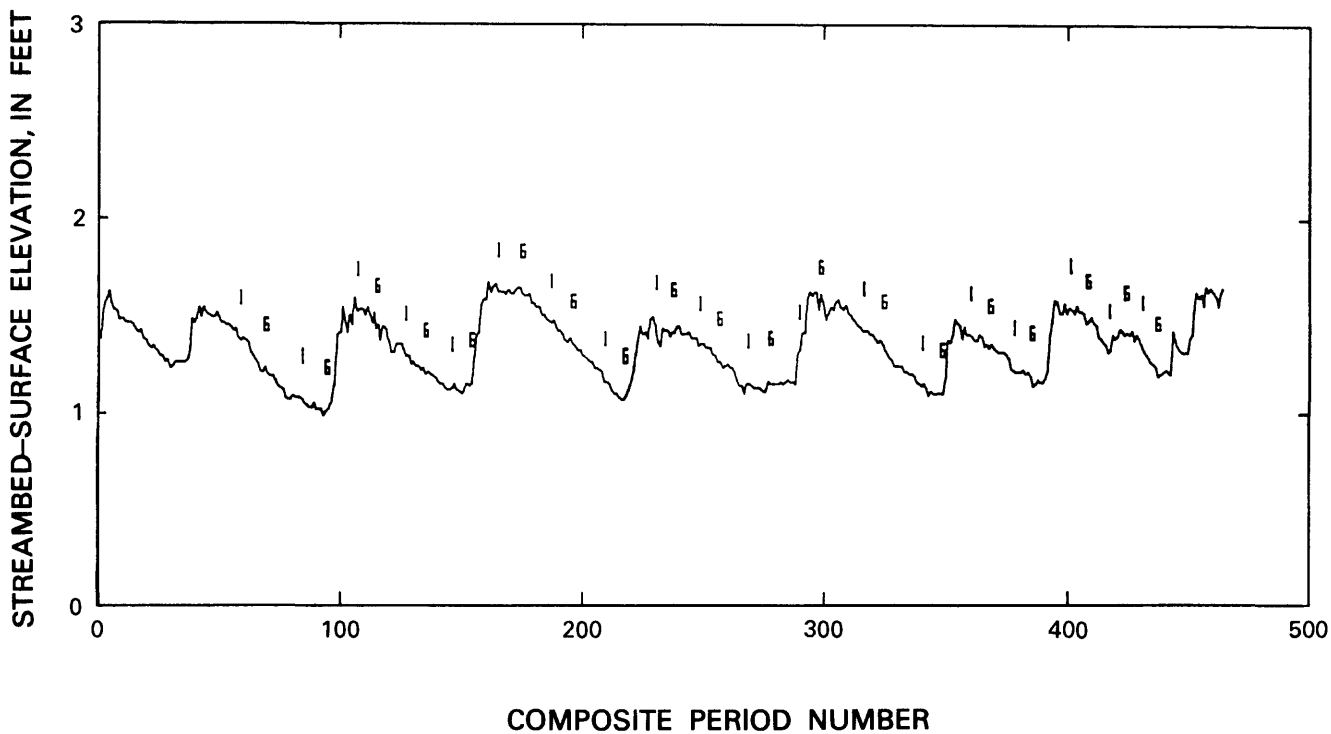


Figure 27. Temporal variation in streambed-surface elevation at the sampling location during run 5 with the 6.5-mm bed material. Sampler numbers superimposed on the streambed-elevation trace show times when samples were collected with the specified sampler. Sampler numbers also infer the relative location of the sampler entrance on the bedform when each sample was collected. The composite-period number expresses elapsed time in terms of composite periods (see p. 9) from an arbitrary initial time.

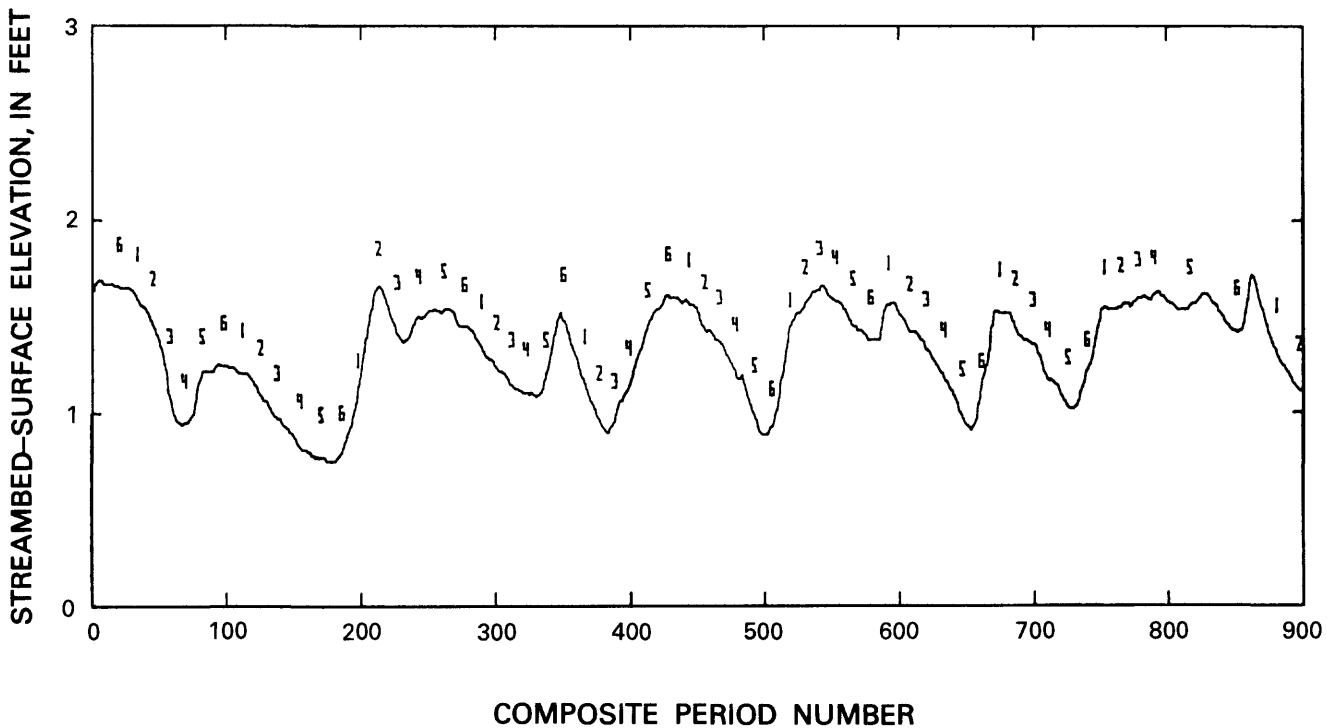


Figure 28. Temporal variation in streambed-surface elevation at the sampling location during run 3 with the 2.1-mm bed material. Sampler numbers superimposed on the streambed-elevation trace show times when samples were collected with the specified sampler. Sampler numbers also infer the relative location of the sampler entrance on the bedform when each sample was collected. The composite-period number expresses elapsed time in terms of composite periods (see p. 9) from an arbitrary initial time.

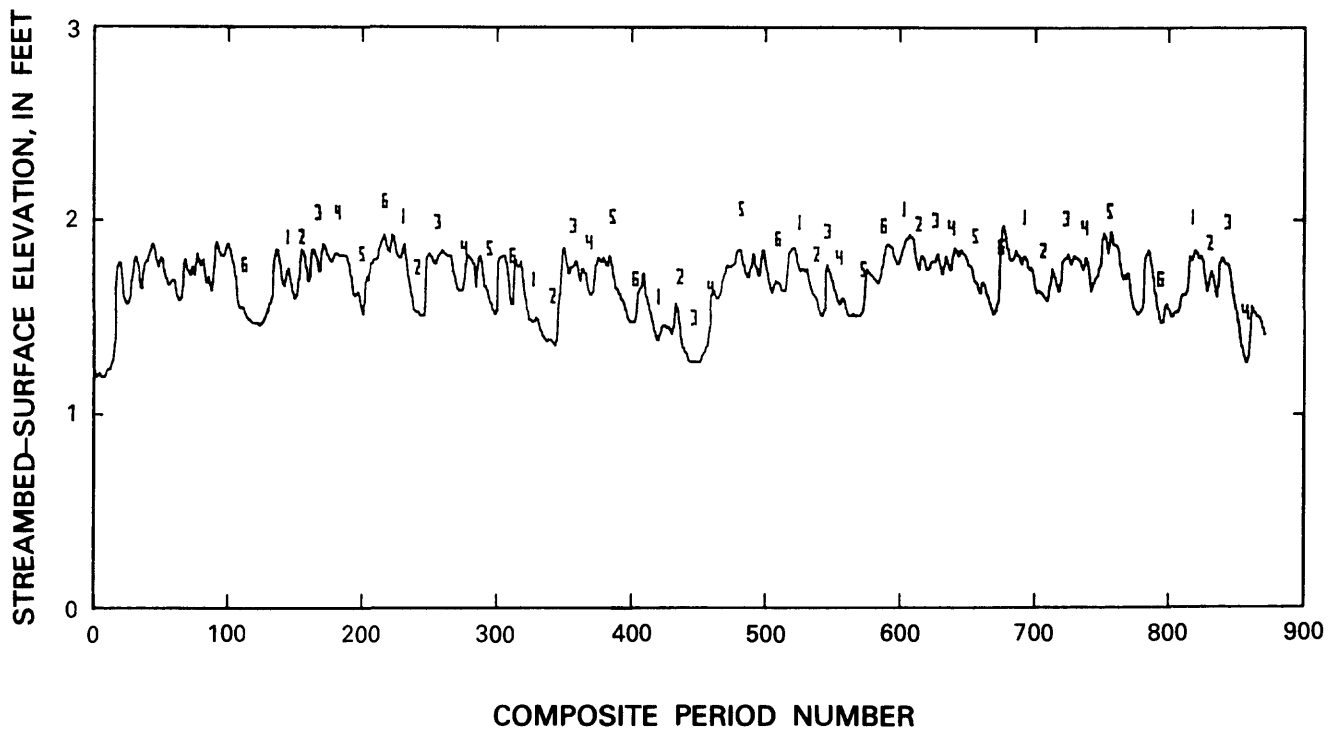


Figure 29. Temporal variation in streambed-surface elevation at the sampling location during run 1 with the 23.5-mm bed material. Sampler numbers superimposed on the streambed-elevation trace show times when samples were collected with the specified sampler. Sampler numbers also infer the relative location of the sampler entrance on the bedform when each sample was collected. The composite-period number expresses elapsed time in terms of composite periods (see p. 9) from an arbitrary initial time.

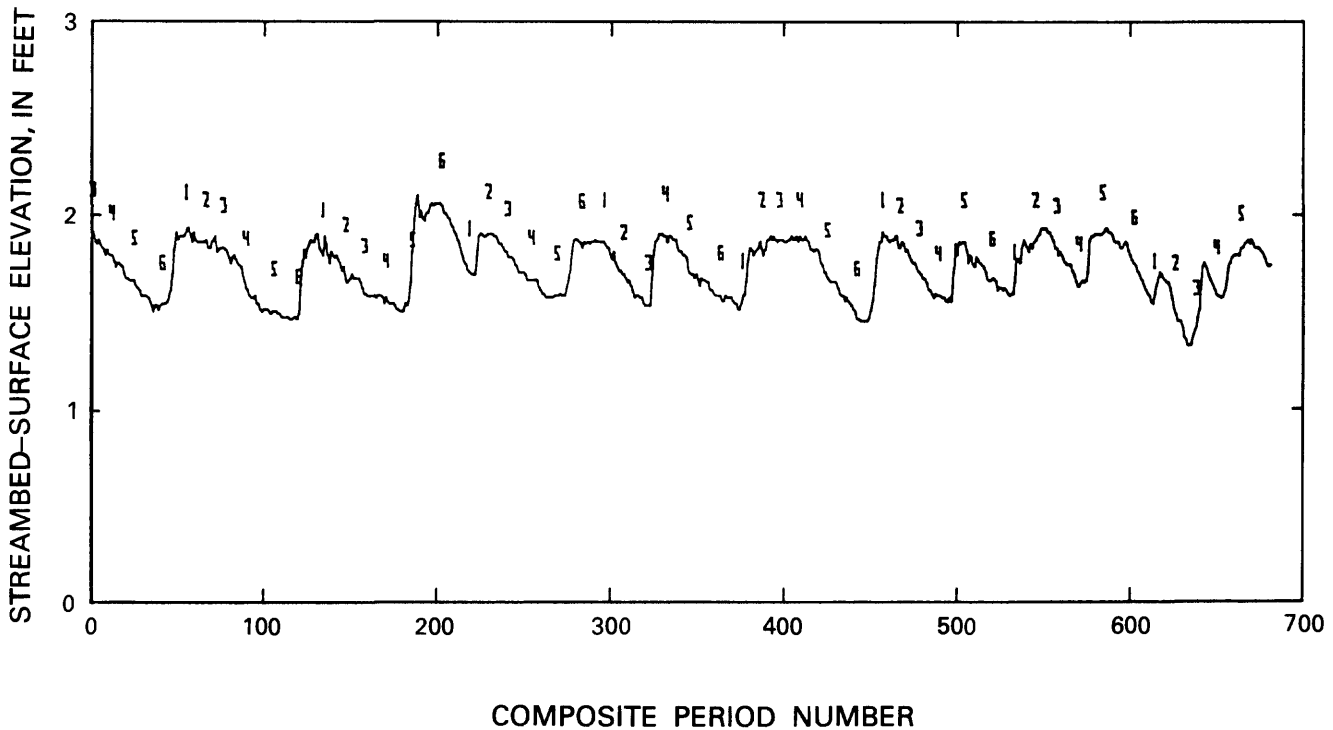


Figure 30. Temporal variation in streambed-surface elevation at the sampling location during run 1 with the bed-material mixture. Sampler numbers superimposed on the streambed-elevation trace show times when samples were collected with the specified sampler. Sampler numbers also infer the relative location of the sampler entrance on the bedform when each sample was collected. The composite-period number expresses elapsed time in terms of composite periods (see p. 9) from an arbitrary initial time.

Table 8. Streambed-surface elevations at fixed locations

[Run numbers appended with a or b designate continuation of the numbered run with a new complement of samplers]

Type of bed material	Run number	Duration of sounding record at indicated longitudinal location (hours)		Data-file name	
		Sampling station ¹	Station 5	Sampling station ¹	Station 5
6.5 mm -----	1	—	—	—	—
	2	—	—	—	—
	2a	—	—	—	—
	3	—	—	—	—
	4	—	—	—	—
	5	12.08	—	SAMPBDEL065R5	—
	5a	11.56	—	SAMPBDEL065R5	—
	6	27.95	—	SAMPBDEL065R6	—
6a	2.12	—	SAMPBDEL065R6	—	
2.1 mm -----	1	42.46	—	SAMPBDEL021R1	—
	2	33.24	—	SAMPBDEL021R2	—
	3	36.32	30.73	SAMPBDEL021R3	STA5BDEL021R3
	4	34.10	32.78	SAMPBDEL021R4	STA5BDEL021R4
	4a	6.48	6.80	SAMPBDEL021R4	STA5BDEL021R4
	5	27.58	24.59	SAMPBDEL021R5	STA5BDEL021R5
	5a	5.32	3.51	SAMPBDEL021R5	STA5BDEL021R5
23.5 mm -----	1	49.66	41.57	SAMPBDEL235R1	STA5BDEL235R1
	2	35.57	32.89	SAMPBDEL235R2	STA5BDEL235R2
	3	34.41	32.25	SAMPBDEL235R3	STA5BDEL235R3
	3a	9.89	5.84	SAMPBDEL235R3	STA5BDEL235R3
	4	22.36	—	SAMPBDEL235R4	—
	5	2.94	3.08	SAMPBDEL235R5	STA5BDEL235R5
Mixture -----	1	36.75	18.88	SAMPBDEL999R1	STA5BDEL999R1
	2	30.90	20.62	SAMPBDEL999R2	STA5BDEL999R2
	3	32.07	30.02	SAMPBDEL999R3	STA5BDEL999R3
	4	5.76	7.76	SAMPBDEL999R4	STA5BDEL999R4
	4a	1.87	2.65	SAMPBDEL999R4	STA5BDEL999R4
	4b	3.87	3.58	SAMPBDEL999R4	STA5BDEL999R4

¹See table 3 for actual longitudinal station.

portant variables, and graphs illustrate the character, range, and variability of elements of the data.

REFERENCES CITED

- Druffel, Leroy, Emmett, W.W., Schneider, V.R., and Skinner, J.V., 1976, Laboratory hydraulic calibration of the Helley-Smith bedload sediment sampler: U.S. Geological Survey Open-File Report 76-752, 63 p.
- Emmett, W.W., 1980, A field calibration of the sediment-trapping characteristics of the Helley-Smith bedload sampler: U.S. Geological Survey Professional Paper 1139, 44 p.
- Helley, E.J., and Smith, Winchell, 1971, Development and calibration of a pressure-difference bedload sampler: U.S. Geological Survey open-file report, 18 p.
- Hubbell, D.W., Stevens, H.H., Jr., Skinner, J.V., and Beverage, J.P., 1985, New approach to calibrating bedload samplers: *Journal of Hydraulic Engineering, Proceedings, American Society Civil Engineers*, v. 111, no. 4, p. 677-694.
- Novak, Pavel, 1957, Bed load meters—Development of a new type and determination of their efficiency with the aid of scale models: Lisbon, International Association of Hydraulic Research, 7th general meeting, Transactions, v. 1, p. A9-1 to A9-11.
- Waterloopkundig Laboratorium, 1949, Bed-load sampler for coarse material "B.T.M. Arnhem": Delft, Holland, Delft Hydraulic Laboratory, Report H1, Code 48.10, 3 p.

Metric Conversion Factors

Inch-pound units used in this report may be converted to SI (International System) units by using the following conversion factors:

Multiply inch-pound unit	By	To obtain SI unit
inch (in.)	25.40	millimeters (mm)
foot (ft)	0.3048	meter (m)
foot per second (ft/s)	0.3048	meter per second (m/s)
cubic foot (ft ³)	0.02832	cubic meter (m ³)
cubic foot per second (ft ³ /s)	0.02832	cubic meter per second (m ³ /s)
pound per second per foot (lb/s/ft)	1.488	kilogram per second per meter (kg/s/m)
ton (t)	0.9072	metric ton (t)